SAFEGUARDS ANALYSIS FOR NEPTUNIUM-237 IN HIGH-LEVEL WASTE THROUGH COMPUTATIONAL AND RADIOCHEMICAL METHODS

A Thesis

By

MARIAH MICHELLE RAMIREZ

Submitted to the Office of Graduate and Professional Studies of
Texas A&M University
in partial fulfillment of the requirements for the degree of

MASTER OF SCIENCE

Chair of Committee,	Sunil Chirayath
Co-Chair of Committee,	Charles M. Folden III
Committee Members,	John Ford
Head of Department,	Michael Nastasi

May 2021

Major Subject: Nuclear Engineering

ABSTRACT

Used nuclear fuel disposition is a major nuclear waste management problem worldwide at the closing end of the nuclear fuel cycle since long-lived actinides can cause safety and criticality concerns. Effective separation of these nuclides can lead to safer storage practices and the establishment of more advanced nuclear material safeguards. In the case of ^{237}Np, which is believed to be weapons useable, little is stated in the International Atomic Energy Agency (IAEA) safeguard protocols.

Neptunium-237 has a fast neutron fission cross section comparable to that of ^{239}Pu, and its production rate is roughly 0.1% of used nuclear fuel. The amount of ^{237}Np produced is low; however, the growing trove of used nuclear fuel is a proliferation risk, especially if the separation of long-lived actinides becomes an industry standard. Production of ^{237}Np was evaluated using ORIGEN2 to simulate one tonne of various fuels for varying reactor types. Burnup simulations comparisons were also made between data points to monitor the overall production for a given reactor. Based on the results, it was determined that a Pressurized Water Reactor (PWR) produced the most ^{237}Np, respectively followed by Boiling Water Reactor (BWR), CANada Deuterium Uranium (CANDU) Reactor, and Fast Breeder Reactor (FBR). These results are further supported by the fact that PWRs and BWRs have a higher ^{235}U content than a CANDU, which burns natural uranium, and FBRs, which burn depleted uranium mixed with plutonium. Comparisons were also made with unique irradiated uranium samples irradiated at the High Flux Isotope Reactor (HFIR) at Oak Ridge National Laboratory (ORNL) and at the Missouri University Research Reactor (MURR). These samples were irradiated at low burnup conditions and experimentally designed to mimic the irradiation of an FBR and CANDU.

Analyses of these samples were completed using inductively coupled plasma mass spectrometry (ICP-MS) to quantify the amount of ^{237}Np in the irradiated samples and to draw conclusions about neptunium production in low-burnup fuels.

DEDICATION

This work is dedicated to my mother and father, Emily M. Ehrlich and Gary W. Ehrlich, and my grandparents, Marcel S. Ramirez-Bice and Bobby J. Bice. Thank you all for your continued support and an unbreakable belief system. I am not sure who I would be or where I would be without your influence throughout my life. Thank you for never allowing me to give up during the tough times or feel discouraged in times of failure. You all have taught me to fight for what I believe in, to stand tall when others wish to see weakness, and most importantly to keep moving forward even if the journey goes unplanned.

Thank you Mom and Dad for helping support me during my undergraduate degree and putting forth military funds to pay for my education. Without this support I would not have been able to attend a top ranked university. Your sacrifices and support mean the world to me. Thank you for teaching me at an early age that working hard can get you places but with education as a stepping stone, it becomes less stressful.

Thank you Grandma and Grandpa for always being there for me during the good and the bad and for always being proud of me even when I was not proud of myself. It means the world to me to have a strong and faithful support system that was always there when I needed them. From bringing me groceries to our long phone calls, I would not be the woman that I am today without your guidance and wise words. You two truly are a Godsend and I am thankful every day for the love, protection, and support you both have always provided me.

This thesis is for you all, may this be representative of my thanks and love for you all. I always hope to make you proud.

ACKNOWLEDGEMENTS

I would like to thank the Department of Nuclear Engineering at Texas A&M University for providing funding during my first-year of graduate school as a Graduate Assistant – Teaching. This opportunity allowed me to further develop my knowledge in nuclear engineering and allowed me to develop a structured communication style to effectively convey ideas to others. This opportunity also provided professional and academic development that I have used throughout my graduate program. The hands-on experience with leading laboratory experiments and office hours has proven to be invaluable and allowed many aspects of my work to be understood in depth.

Within the Department of Nuclear Engineering at Texas A&M, I would like to thank the Center for Nuclear Security Science and Policy Initiatives (NSSPI) and the department staff for providing me the support I needed to conduct my research, as well as providing nonproliferation courses to further expand my knowledge. Thank you for being so patient and willing to guide me throughout this journey.

I would like to thank my committee chair and co-chair, Dr. Sunil S. Chirayath and Dr. Charles M. Folden III, for their guidance and support throughout the course of my research and coursework. Their academic supervision has provided me with knowledge from a wide range of classes from radiochemistry to nonproliferation courses. Thank you for funding this research, my coursework, and granting me opportunities to speak about my work throughout my three years at Texas A&M. I would also like to thank my committee member, Dr. John Ford for participating in this research and assisting me throughout my time at Texas A&M.

I would like to thank the Nuclear Science and Security Consortium (NNSC) under the National Nuclear Security Administration (NNSA) for their constant support and outreach during

this research. Thank you and Dr. Folden for providing me funding (tuition, health insurance, stipend, and travel…) under the Cyclotron Institute at Texas A&M University and for providing me with a mentor at Los Alamos National Laboratory (LANL). Without the support of the Cyclotron Institute and the NSSC I would not be in the position that I am in today or have the lengthy experience and comprehension of nuclear engineering concepts, radiation detection, and radiochemistry.

I would like to thank Los Alamos National Laboratory (LANL) for allowing me to complete two summer internships under the mentorship of Mr. Alex McSpaden, Dr. Rene Sanchez, and Mr. Jesson Hutchinson with the Advanced Nuclear Technologies (NEN-2) Division. Thank you for mentoring me and providing me opportunities to conduct research within the field of nuclear engineering. Working within NEN-2 has provided me several professional relationships and friendships that I will be forever thankful for.

I would like to thank Dr. Jeremy Osborn and Dr. Braden Goddard for their Ph.D. dissertation works whose previous research provided me a starting ground to expand and produce my own thesis work. This work provided insight to what work had previously been done regarding neptunium and a good background on irradiated material that were imperative to my work.

Thanks also to my friends and colleagues for your constant encouragement and support throughout this process and for making my time at Texas A&M University a memorable experience. I would like to specifically thank Dr. Athena Sagadevan, Ernesto Ordoñez, Jeremy King, Veronica Ordoñez, Juliann Lamproe, and Kristin Smith for always providing listening ears, moral support, helpful advice, problem-solving and brainstorming capabilities, and most of all their friendship throughout this time. The five of you, amongst many others, are the reason I am able to complete this degree with such success and enjoyment. Finally, thanks to my loving

family for their encouragement and their patience and love throughout this process; you have always provided me a listening ear and helpful hand to stand back up and keep going. Words cannot express how thankful I am for everyone who has helped me throughout my time at Texas A&M University. Last but certainly not least, I would like to thank my four-legged best friends, Cookie and Pancake, for all of the cuddles, unconditional love, tail wags, smiles, and laughs that they have provided me over the past few years. Words cannot express how much the two of them have helped me.

Thank you to all who had a part in making this possible.

CONTRIBUTORS AND FUNDING SOURCES

Contributors

This work was supervised by a thesis committee consisting of Professor Sunil Chirayath, Professor Charles M. Folden III, and Professor John Ford who served as advisor, co-advisor, and committee member, respectively: Professor Sunil Chirayath and Dr. John Ford of the Department of Nuclear Engineering and Professor Charles M. Folden III of the Department of Chemistry and Cyclotron Institute.

The data analyzed for section 3 were provided by Dr. Jeremy Osborn who modeled the HFIR and MURR irradiation models in MCNP; this work is referenced below. A portion of the results were collected by Dr. Brent Miller who conducted ICP-MS analysis due to COVID-19 laboratory restrictions. Samples were prepared by the student independently.

All other work conducted for the thesis was completed by the student independently.

Funding Sources

This material is based upon work supported by the Department of Energy National Nuclear Security Administration through the Nuclear Science and Security Consortium under Award Number(s) DE-NA0003180 and/or DE-NA0000979.

This report was prepared as an account of work sponsored by an agency of the United States Government. Neither the United States Government nor any agency thereof, nor any of their employees, makes any warranty, express or implied, or assumes any legal liability or responsibility for the accuracy, completeness, or usefulness of any information, apparatus, product, or process disclosed, or represents that its use would not infringe privately owned rights. Reference herein to any specific commercial product, process, or service by trade name, trademark, manufacturer, or otherwise does not necessarily constitute or imply its endorsement, recommendation, or favoring

by the United States Government or any agency thereof. The views and opinions of authors expressed herein do not necessarily state of reflect those of the United States Government or any agency thereof.

Section 4 was partially funded by Los Alamos National Laboratory and was conducted to fulfill the student's internship work plan while mentored by Alex McSpaden, Rene Sanchez, and Jesson Hutchinson.

NOMENCLATURE

Am	Americium
AmLi	Americium-lithium
AWCC	Active Well Coincidence Counter
BWR	Boiling Water Reactor
CANDU	CANada Deuterium Uranium
Cm	Curium
cm	Centimeter
DAF	Device Assembly Facility
ENMC	Epithermal Neutron Multiplicity Counter
Eq	Equation
FBR	Fast Breeder Reactor
FSV	Flow Sheet Verification
g	Gram(s)
GADRAS	Gamma Detector Response and Analysis Software tool
Gd	Gadolinium
Gd_2O_3	Gadolinium(III) oxide
GWd	Gigawatt-day
H_2O_2	Hydrogen peroxide
He	Helium
HBr	Hydrogen bromide
HCl	Hydrogen chloride
HDEHP	Di-(2-ethylhexyl) orthophosphoric acid

HEU	Highly Enriched Uranium
HFIR	High Flux Isotope Reactor
HNO_3	Nitric acid
HPGe	High-purity Germanium Detector
IAEA	International Atomic Energy Agency
ICP-MS	Inductively Coupled Plasma Mass Spectrometry
k’	Retention factor or capacity factor
keV	Kiloelectron volt
kg	Kilogram
LANL	Los Alamos National Laboratory
LN	LaNthanides Resin
Ln	Lanthanide
M	Molar
MCNP6/6.2	Monte Carlo N-Particle Transport code, version 6/6.2
MeV	Megaelectron Volt
min	Minute
mL	Milliliter
mm	Millimeter
mol	Mole(s)
MTU	Metric Tonne of Uranium
MURR	Missouri University Research Reactor
MWd	Megawatt Day
MWd/MTU	Megawatt Day per Metric Tonne of Uranium

n	Neutron
NEN-2	Advanced Technologies Group
NeSO	Neptunium Subcritical Observation
NH_2OH	Hydroxylamine
$(NH_4)_2C_2O_4$	Ammonium Oxalate
NNSA	National Nuclear Security Administration
NoMAD	LANL Neutron Multiplicity ^{3}He Array Detectors
Np	Neptunium
NSSC	Nuclear Science and Security Consortium
NSSPI	Center for Nuclear Security Science and Policy Initiatives
O	Oxygen
OD	Outer diameter
ORNL	Oak Ridge National Laboratory
Pa	Protactinium
ppb	Parts per Billion
ppm	Parts per Million
Pu	Plutonium
PUREX	Plutonium Uranium Recovery by EXtraction
PWR	Pressurized Light Water Reactor
s	Second(s)
SNM	Special nuclear material
$T_{1/2}$	Half-Life of Isotope
TAMU	Texas A&M University

TBP	Tributyl phosphate
U	Uranium
UO_2	Uranium-dioxide
UTEVA	Uranium and TEtraValents Actinides resin
wt%	Weight percent
yr	Year(s)
(α,n)	Alpha-neutron
β	Beta particle
γ	Photon
°C	Celsius
μm	Micrometer
μL	Microliter
$\bar{\upsilon}$	Nubar
%	Relative error represented in percent

TABLE OF CONTENTS

LIST OF FIGURES

LIST OF TABLES

1. INTRODUCTION

Used nuclear fuel, or material irradiated in a nuclear reactor, is a major nuclear waste management problem worldwide when trying to close the nuclear fuel cycle due to the inherent proliferation risks posed by large troves of this material. The global stockpile of spent nuclear fuel consists of nuclear materials such as highly enriched uranium (HEU) and plutonium, which are weapons useable, along with minor actinides and fission products. [1] The separation of long-lived minor actinides, such as neptunium (Np) and americium (Am), and major actinides, such as uranium (U) and plutonium (Pu), could lead to safer storage practices and allow for advanced nuclear material safeguards methods to be implemented. [2]

The purpose of safeguard measures is to ensure the timely detection of diverted special nuclear material (SNM) by a State. [3] By nature, safeguard measures are not designed to be 100% effective in the detection of diverted nuclear material but rather make diversion more difficult and costly so that a State or adversary would not attempt it. [3] An adversary can be defined as a person with malicious intent and acts that can be harmful to a facility or State. [4] Safeguards work hand-in-hand with nuclear forensics, which is a useful tool when identifying nuclear material with high-confidence intervals. [1] Nuclear forensic work is often exhibited in radiochemical separations that utilize mass spectrometry to determine isotopes present in low concentrations. Mass spectrometry is more sensitive than alpha or gamma spectrometry because the detection limits are significantly lower than other methods, with identification capabilities as low as tens of attograms. [5] In the realm of nuclear forensics and low concentration samples this form of destructive analysis provides a detailed analysis of the constituents present within a sample.

Although separation chemistry on the nuclear fuel cycle is performed only in the United States by the military, neptunium is not safeguarded because it is rarely separated from used fuel. [4] This is also true for countries engaged in used fuel reprocessing in their civilian and military fuel cycles. The International Atomic Energy Agency (IAEA) adopted statutes declaring that neptunium was not in large enough abundance to be of concern. [6, 7] Currently, there are no safeguard methods under the IAEA in place for ^{237}Np; however, literature suggests that it needs to be considered as separation methods and technology improve along with a growing inventory of nuclear waste. [3]

The purpose of the study presented is to evaluate the separation of ^{237}Np to quantify the amount of neptunium present in high-level radioactive waste remaining after separation of plutonium and uranium. A literature review was conducted to assess the separation of neptunium from plutonium, uranium, fission products, and americium and will be discussed in section 1.2. [2, 8-10]

1.1 Introduction to Safeguard Practices and Neptunium Production

Fuel reprocessing in the civilian nuclear fuel cycle is not utilized in the United States due to President Carter banning commercial reactor fuel reprocessing on April 7, 1977. The key issue driving this policy was the risk of nuclear weapons proliferation by plutonium diversion from the civilian fuel cycle, and to encourage other nations to follow the United States. However, Russia, France, the U.K., Japan, Pakistan, North Korea, and India continue to reprocess spent nuclear fuel. Evaluation of the nuclear fuel reprocessing by the International Atomic Energy Agency (IAEA) safeguards is a voluntary offer safeguards agreement for the weapons states. Most of the IAEA safeguards efforts at a reprocessing facility are to account for and control plutonium, which forms about 1% of the mass remaining in used nuclear fuel. However, other transuranic

elements, especially neptunium, can also be used for producing a nuclear weapon. [3] The amount of neptunium produced is approximately 0.1% of the used nuclear fuel.

It is worth mentioning that in used nuclear fuel reprocessing facilities, plutonium and uranium are recovered. Fission products and neptunium become part of high-level radioactive liquid waste, which in some countries are immobilized into vitrified solid waste. Hence, in countries practicing reprocessing, neptunium is present in the high-level radioactive waste. The amount of ^{237}Np produced is low, but the growing abundance of used nuclear fuel is a proliferation risk due to its weapons-use capabilities. Another fact is that plutonium in used fuel is not weapons-useable material because ^{239}Pu is the requisite material for weapons. However, other less-favorable plutonium isotopes (^{238}Pu, ^{240}Pu, and ^{242}Pu) are also present in appreciable quantities. Neptunium-237 has a fast neutron fission cross section comparable to ^{239}Pu, and therefore has a similar suitability for use in nuclear weapons. This creates a real concern since neptunium is not currently under safeguards, either in present reprocessed waste or in used fuel.

The IAEA recognized that neptunium can be used to develop a weapon, which resulted in an unofficial monitoring system to be implemented to assess if neptunium has been separated; however, due to IAEA rule-enforcing limitations official neptunium safeguards have not been implemented. There is no material balancing period, or the time between two consecutive inventory measurements [11], in place for neptunium, and thus there are no safeguard measures. However, the current monitoring system in place determines if large-scale separation has occurred. [12] If large-scale neptunium separation is detected, this could be further proof that an investigation is required and safeguard measures established for neptunium. The current method of tracking is called flow sheet verification (FSV) which is based on a ratio method of neptunium

to other high concentration species in the major output streams. If the ratio results are not as expected it implies that separation has occurred within the system. [12]

Neptunium is present in nature as a direct result of neutrons producing transmutation reactions in uranium ores and can also be produced in nuclear power reactors. [7] The specific isotope of concern is ^{237}Np due to its fast neutron fission cross section comparable to that of ^{239}Pu. There are two plausible paths through which ^{237}Np can be produced in nuclear fuel, as shown in Eq.1: (1) successive neutron capture of ^{235}U and ^{236}U ending in ^{237}U which beta decays to ^{237}Np; (2) when a fast neutron occasionally liberates a neutron from ^{238}U to produce ^{237}U which then beta decays to ^{237}Np, as shown in Eq. 1:

$$^{235}\mathrm{U}(n,\gamma)^{236}\mathrm{U}$$
$$^{236}\mathrm{U}(n,\gamma)^{237}\mathrm{U} \rightarrow \beta \rightarrow {}^{237}\mathrm{Np} \quad \text{Eq. 1.}$$
$$^{238}\mathrm{U}(n,2n)^{237}\mathrm{U} \rightarrow \beta \rightarrow {}^{237}\mathrm{Np}$$

Open literature suggests the bare critical mass, defined as the minimum amount of fissile material needed to make a weapon, of ^{237}Np is 60 kg as compared to 10 kg for ^{239}Pu. [13, 14] The critical mass of ^{237}Np was determined at Los Alamos National Laboratory (LANL) by placing a 6 kg bare sphere of ^{237}Np within two hemispheres of highly enriched uranium shells. The thickness of these shells was increased over time by using additional concentric shells of the same material to determine the final suggested critical mass of 60 kg. It is worth noting that the neptunium sphere used for this calculation was not 100% pure ^{237}Np. Chemical analysis was performed on the neptunium sphere's sprue, the results of which are shown in Table 1. Approximately 1% of the mass of the total sphere contents are not accounted for due to the sprue sample not dissolving to completeness. [13]

Table 1. The chemical analysis performed at LANL results for the neptunium sphere. The elemental breakdown by weight percent for a given nuclide. [13] Approximately 1% of the mass of the total sphere contents are not accounted for due to sprue not dissolving to completeness. [13]

Element	Fraction (wt. %)	Nuclide	Abundance (wt. %)
Np	98.8	^{237}Np	100
Total U	0.035	^{233}U	9.92
		^{234}U	1.61
		^{235}U	79.2
		^{236}U	0.44
		^{238}U	8.74
Total Pu	0.0355	^{238}Pu	4.45
		^{239}Pu	88.18
		^{240}Pu	6.32
		^{241}Pu	0.17
		^{242}Pu	0.89
Am	Trace	^{241}Am	6.0 ppm
		^{243}Am	1823.0 ppm

1.2 Radiochemical Separation Methods for Neptunium and Analysis

The separation of neptunium from other elements is a difficult process because it extracts with Pu, a major actinide, that is high abundance compared to Np. [2, 10, 15-18] To get effective separation of neptunium from other nuclides in nuclear waste, several methods have been implemented. Some methods have explored the reduction of plutonium and neptunium's oxidation states using various agents to promote extraction from various mixtures of actinides. A common separation scheme is a modified plutonium uranium reduction extraction (PUREX) process and the use of column chromatography. The following sections outline the PUREX process, a modified PUREX process, and define column chromatography.

1.2.1 Uranium and Plutonium extraction with the PUREX process [19]

The PUREX process was developed at the Knolls Atomic Power Laboratory and tested at Oak Ridge. In 1954, the PUREX process was adopted by the Savannah River Plant and replaced

previously utilized methodologies due to its effectiveness in separating U and Pu from fission products and minor actinides. [19] The PUREX process steps are outlined below:

1. Spent nuclear fuel is chopped and dissolved. After this, feed conditioning is done with sodium nitrate to adjust the oxidation state of Pu to Pu(IV).
2. Tributyl phosphate (TBP) and kerosene are added to the mixture and vigorously stirred in a mixer settler or pulsed column. This creates two distinct phases: (1) an aqueous phase with fission products and trace amounts of actinides and (2) an organic phase with the actinides, Pu and U. This step causes separation of the organic phase, containing Pu and U, from minor actinides such as Np, Am, and Cm. In 4 M nitric acid, Np, Am, and Cm separate out and go into the raffinate, otherwise known as the waste stream.
3. Ferrous sulfamate dissolved in nitric acid (HNO_3) is added to the organic phase to reduce the oxidation state of Pu from Pu(IV) to Pu(III). This creates a new aqueous phase and allows Pu to back-extract into the aqueous phase.
4. Purification of Pu from U and trace amounts of the fission products occurs in the separation caused by the reduction of Pu.
5. Uranium is then extracted from the organic phase and purification of U from the remaining amount of trace fission products occurs. This step can be done by stripping the UO_2 with 0.1 – 1 M HNO_3. This dilutes it and back-extracts the U into a new aqueous phase.
6. Repeat all steps at least three or four times to achieve high purification yield.

The standard PUREX process outlined above can be modified in order to separate out Np, Am, and Cm from the raffinate which results from the PUREX process. This process is detailed in section 1.2.2 and outlined in steps 1-3, below.

1.2.2 Separating Np, Am, and Cm from the raffinate resulting from the PUREX process

1. Np can be separated from Am and Cm by the reduction of Np(V) to Np(IV). TBP and kerosene are utilized to extract Np from Am and Cm, which stay in the aqueous phase, because it forms an even complex with the TBP. This is extractable.
2. Back-extraction of Np(IV) can occur by oxidizing Np(IV) to Np(V). This oxidation occurs in 0.1 – 1 M HNO_3. This back-extracts into a clean aqueous phase.
3. Next, di-(2-ethylhexyl)orthophosphoric acid (HDEHP) can be used to extract Am and Cm from the aqueous phase. HDEHP is an organophosphorous compound that is useful when separating lanthanides from actinides, thus resulting in the separation of Am from the Cm so further purification can be done. [19, 20]

This modified process takes the raffinate, the result of the waste stream from the PUREX process, and further purifies it. This is helpful in the separation of long-lived minor actinides from major actinides and could allow for advanced nuclear material safeguards methods to be implemented. [2]

1.2.3 Column Chromatography & Analysis with Inductively Coupled Plasma Mass Spectrometry (ICP-MS) [21]

Column chromatography is a form of destructive analysis in radiochemistry that separates individual components of a complex mixture, such as minor and major actinides in used nuclear fuel, with a stationary phase and mobile phase. A stationary phase is a phase that allows the mobile phase to pass through without interaction. Using these two phases, the solutes can be identified and quantified using alpha and gamma spectroscopy, mass-spectroscopy, among other analytical methods once separation occurs. A solute is a substance that can be dissolved into another substance, which is known as a solvent. The separation in column chromatography is

caused by intermolecular interactions with the stationary phase or mobile phases within a column. These intermolecular interactions dictate how quickly or slowly a solute will elute, meaning separation and removal of constituent in the sample, from a column. A visual, step-by-step, representation of how column chromatography works can be seen in Figure 1, below.

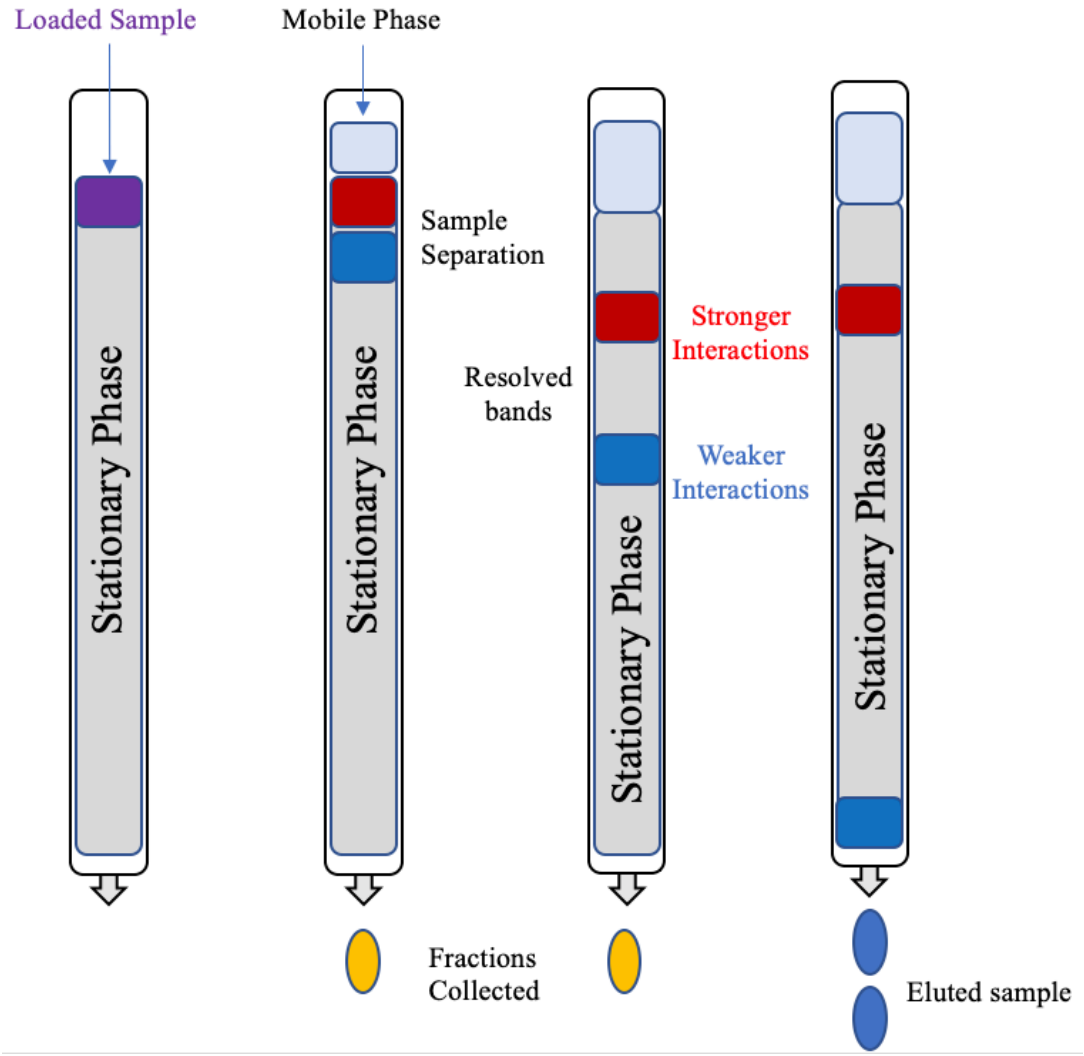

Figure 1. A step-by-step visual representation of column chromatography.

The construction of a column when packing the stationary phase directly impacts the resolution of the bands, which improves separation of the sample constituents if properly prepared. A column is first loaded with a stationary phase and then the desired sample is loaded

with a known, discrete volume to the head of the column (top of the column). A mobile phase is injected to the column, controlled by some flow rate continuously for so many bed volumes, to begin separation of the loaded sample. A bed volume is defined by the amount of packed material is in the stationary phase; it is common to use a mobile phase, or rinse state, that is larger than the bed volume. Mobile phases can be liquid or gas, but need to have a viscosity that allows the eluents to be pushed through the stationary phase. The rate at which elution occurs is dictated by the intermolecular interactions between the eluent and stationary phase as well as the concentration of the mobile phase. As the mobile phase is continuously injected into the column the solutes are continuously partitioned, where these are referred to as eluents that are eluted off of the column.

The rate of partitioning is controlled by the eluent's affinity for the stationary phase, s, or the mobile phase, m. It will elute faster if the constituents' affinity for the mobile phase is higher than the stationary phase and will elute slower if the affinity for the stationary phase is higher than that of the mobile phase. The rate at which eluents are eluted is dictated by a distribution coefficient, Eq. 2.

$$K = \frac{[A]_s}{[A]_m} \quad \text{Eq. 2}$$

Where *A* represents a specific analyte in a particular phase, s represents the stationary phase, and m is indicative of the mobile phase. A higher distribution coefficient, *K*, can be achieved through repeated separations. The time an eluent spends in each phase is determined using Eq. 3, which determines the retention time.

$$t_r = t_s + t_m \quad \text{Eq. 3}$$

The total retention time is the sum of the time the eluent spends in each phase where t_s represents the time spent in the stationary phase and t_m represents the time spent in the mobile phase. The retention time can then be utilized to determine a retention factor, Eq. 4.

$$k' = \frac{t_r - t_m}{t_m} = \frac{t_s}{t_m} \quad \text{Eq. 4}$$

In the case of k', t_m is the amount of time it takes the mobile phase to flow from the head of the column to the end of the column. This can be referred to as the dead-time or hold-up factor of a column. k' is the ratio of time a molecule spends absorbed to the stationary phase relative to the amount of time it spends in the mobile phase. This relationship is indicative of how long an eluent spends in a phase. A higher k' indicates more time was adsorbed to the stationary phase, whereas a lower k' indicates more time in the mobile phase. Eq. 4 can be further expanded to evaluate the number of moles that are present in a given phase, as shown in Eq. 5.

$$k' = \frac{t_r - t_m}{t_m} = \frac{t_s}{t_m} = \frac{n_s}{n_m} \quad \text{Eq. 5}$$

The retention factor can be further rewritten in terms of the number of the moles or molecules in the stationary phase or in the mobile phase, n_s and n_m, respectivelty, which can then be used to evaluate the molar concentration of an eluent.

$$k' = \frac{[\frac{n_s}{V_s}]V_s}{[\frac{n_m}{V_m}]V_m} = \frac{[A]_s V_s}{[A]_m V_m} = \mathrm{K}\,(\frac{V_s}{V_m}) = \frac{K}{\beta} \quad \text{Eq. 6}$$

$$\text{Where, } \mathrm{K} = \frac{[A]_s}{[A]_m} \text{ and } \beta = \frac{V_m}{V_s} \quad \text{Eq. 7}$$

Molar concentration can be written as $\frac{n_i}{V_i}$ which is the number of moles or molecules in a given volume of a specific phase. The phase ratio, β, is defined as $\frac{V_m}{V_s}$ which can be used to determine the overall retention factor.

The eluted molecules can be further analyzed using inductively coupled plasma mass spectrometry (ICP-MS). ICP-MS utilizes coupled plasma to ionize the loaded sample and analyze/identify constituents in a sample with great speed, sensitivity, and precision. This is useful for nuclear forensics because this equipment offers high-precision in its identification of isotopes. This can be used to detect metals, non-metals, and different isotopes of the same element in dissolved, liquid samples in low concentrations.

1.3 HFIR and MURR Pellet Irradiations[1]

Radiochemical separations are useful in determining the constituents of a known sample and applicable to nuclear forensics. At Texas A&M University (TAMU), two uniquely irradiated uranium samples exist within the Department of Nuclear Engineering that allow for radiochemical separation methodologies to be developed and tested as well as numerous nuclear forensics methods utilizing computational capabilities. [22-27]

Irradiations of depleted uranium dioxide fuel samples were done in the High Flux Isotope Reactor (HFIR) at Oak Ridge National Laboratory (ORNL) by Texas A&M University [28] to a burnup of approximately 5 GWd/MTU. The *MCNPX* model resulted in a full burn of 4310 MWd/MTU where ORNL reported 4270 MWd/MTU. [28] The *MCNPX* model of the irradiation capsule and HFIR can be seen in Figures 2 and 3. The irradiation was done under specific conditions to resemble a Fast Breeder Reactor (FBR) and to monitor the production of weapons-grade Pu; however, this sample has other significant nuclear forensic characteristics that will be discussed in later chapters. The depleted uranium dioxide irradiation was carried out in a pseudo-

[1] Figures 2 and 3 are reprinted with permission from Taylor & Francis Group to use images from "Experimental and Computational Forensics Characterization of Weapons-Grade Plutonium Produced in a Fast Reactor Neutron Environment by Mathew W. Swinney, *et. al.* Copyright 2017 by Nuclear Technology. Figure 4 is reprinted with permission from Elsevier Permissions Helpdesk to use image from "Computational and experimental forensics characterization of weapons-grade plutonium produced in a thermal neutron environment" by Jeremy M. Osborn, *et. al.* Copyright 2018 by Elsevier.

fast neutron environment through the use of a capsule made of gadolinium (Gd). Gadolinium was utilized as a thermal neutron shield, ultimately decreasing the number of thermal neutrons and maximizing the fast-to-thermal ratio [28], at least until the isotopic distribution of the Gd had changed due to its burnup.

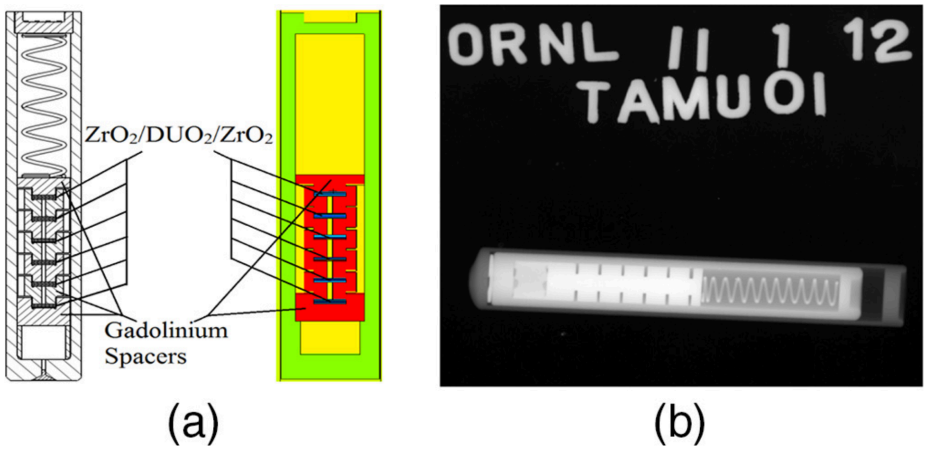

Figure 2. (a) *MCNPX* schematic model of the irradiation capsule compared to (b) a radiograph of the capsule prior to its irradiation. [28]

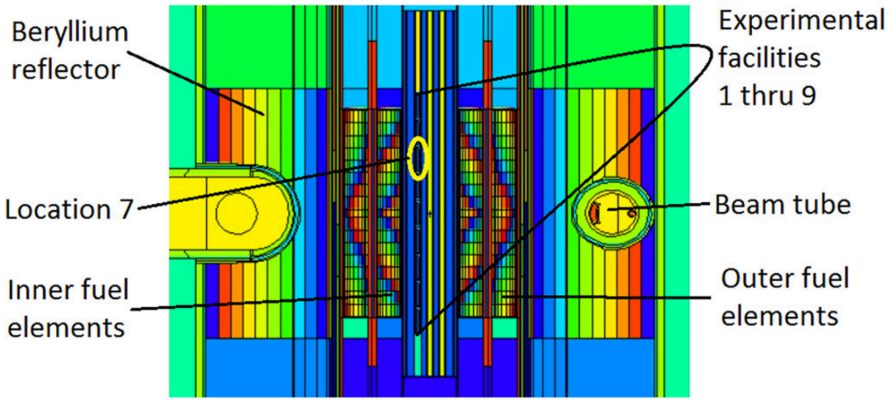

Figure 3. The *MCNPX* model of HFIR that shows the irradiation capsule location highlighted and labeled 'Location 7'. [28]

Complementary to this work, an irradiation of natural uranium fuel samples was carried out by Texas A&M University at the Missouri University Research Reactor (MURR) to support

further analysis for the production of weapons-grade plutonium. [26] The *MCNP*®[2]6 model of one-eighth of the MURR core can be seen in Figure 4. [29, 30] Due to symmetry, one-eighth of the core was sufficient for model and simulating purposes. This irradiation was done under specific conditions to resemble a CANDU reactor. The natural uranium fuel samples were irradiated to a burnup of 0.973 ± 0.032 GWd/MTU within the graphite reflector region surrounding the MURR core. [26]

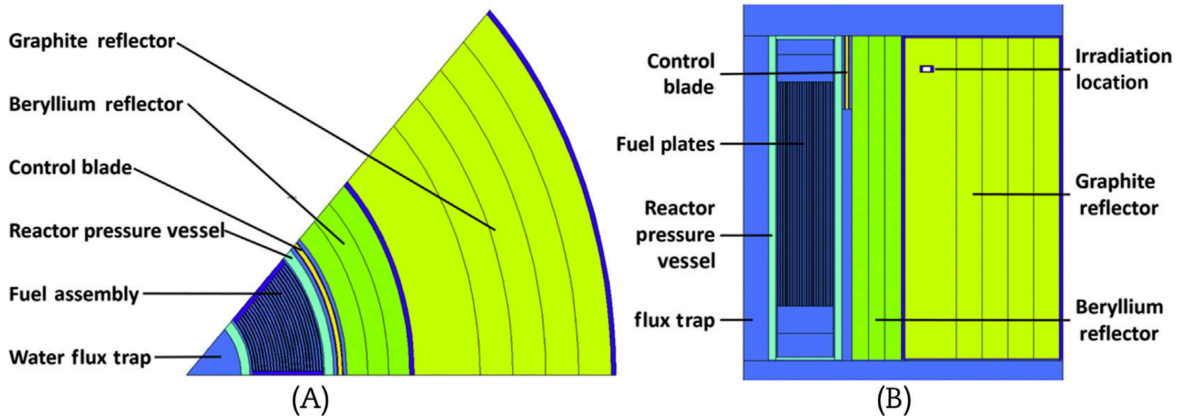

Figure 4. A *MCNP*®6 one-eighth core model of MURR where (A) is the radial cross-section of one-eighth of the core and (B) is the axial cross-section of one-eighth the core that highlights the irradiation location.

Computational simulations were performed in conjunction with the experimental components to validate results and to investigate the concentration of actinides and fission products produced in a natural uranium fuel as a function of decay time and irradiation time. [26, 28] Computational simulations were conducted utilizing *MCNP*®6/6.2 and the simulation results were used to analyze the amount of a given actinide after various fuel burnup time steps. In this thesis work, radiochemical analyses were performed on the uranium samples that were irradiated at HFIR and

[2] ***MCNP®*** and ***Monte Carlo N-Particle®*** are registered trademarks owned by Triad National Security, LLC, manager and operator of Los Alamos National Laboratory (LANL).

MURR, and the results derived from the reactor core simulations from Texas A&M's HFIR and MURR irradiations were analyzed.

Previous work concerning the quantification of neptunium in irradiated fuel consisted of developing a technique utilizing detector response values from active and passive measurements to determine the masses of neptunium, uranium, plutonium and americium. [6] Measurements were completed using Active Well Coincidence Counter (AWCC) and Epithermal Neutron Multiplicity Counter (ENMC) with various (α,n) sources and actinide materials. [6] For the neptunium measurement to be obtained, the following steps were executed in Dr. Braden Goddard's work to determine the elemental masses mentioned above. [6] Passive measurements were taken of an irradiated sample and then analyzed using neutron multiplicity methods. The first step in Dr. Goddard's work quantified the amount of plutonium and americium present in a sample. If a sample is shown to include uranium, plutonium, and americium, or neptunium, plutonium, and americium the mass of uranium and neptunium could be determined by the summation of the worth constant for an americium-lithium (AmLi) neutron source measurement for a given isotope multiplied by the respective mass of a given nuclide. The worth constant utilizes a relationship between ^{239}Pu, the AmLi source, and the isotope of interest to give the equivalent worth constant for that isotope. If a sample consists of both uranium and neptunium, then further measurements need to be taken with a second active measurement and then solved using a system of equations determined for a given nuclide. [6]

1.4 Scope

Neptunium is not separated from uranium and plutonium in spent fuel reprocessing, instead Np goes into the waste stream. Accumulation of ^{237}Np is a problem as the grove of waste increases. Currently ^{237}Np is not explicitly safeguarded but has been acknowledged as a

potential weapons-use material by the IAEA. The task was to identify how much ^{237}Np is produced by nuclear reactors to then determine how much is present in the waste stream from a given throughput of fresh fuel. This was done using computational methods and then verified using radiochemical experimental methods.

To check the computational methods, experimental methods were done to separate Np from the waste stream of HFIR and MURR irradiated depleted and natural uranium samples, respectively. This analyses can help determine how much ^{237}Np is present in used nuclear waste and help draw conclusions if this is comparable to the significant quantity posed by LANL.

2. METHODOLOGY

2.1 Column Chromatography Radiochemical Separations to Isolate ^{237}Np

2.1.1 Construction of a Column for Column Chromatography

The purpose of performing radiochemical separations was to physically quantify how much neptunium would be present in an irradiated uranium sample. Radiochemical separation would result in the separation of the major actinides and transuranium isotopes such as uranium, plutonium, and neptunium. The construction of a column is crucial to the usefulness of a column and directly impacts the overall separation of the eluents. The construction of a column is as follows:

1. A column, with a circle piece of Teflon at the bottom, is first loaded with a stationary phase. For the purpose of this work, a DOWEX 1x8 resin with 100 – 200 mesh size was used. This resin was chosen due to Pu having a high affinity in 8 M HNO_3 while Np, Am, fission products, and U have low affinity. [10] The DOWEX 1x8 resin was loaded into the column using a slurry mixture until a 1 mL bed was compacted. A slurry mixture is a wet mixture comprised of water and the chosen resin which permits the slurry to freely move within the column and allows for the resin to compact evenly while minimizing air bubbles or discrepancies, which can heavily impact the yield of a column.
2. Once the resin in compacted, quartz wool was added to the column and used to push down the resin layer and form a boundary for the loaded sample.
3. The column was conditioned using rinse states of the acid concentration, in this case 8 M HNO_3, in order for the resin to be fully immersed with the appropriate concentration of the mobile phase. Conditioning the column flushes out residual contaminants and ensures the column is reliable to use for separation chemistry.

4. The sample, dissolved HFIR or MURR irradiated material, was loaded at a known, discrete volume to the head of the column on top of the quartz wool.
5. A mobile phase was injected to the column, controlled by some flow rate continuously for a set amount of bed volumes, and dictated by the intermolecular interactions and concentration. The flow rate was controlled by gravity for the duration of this work.
6. As the mobile phase is continuously injected into the column the solutes are continuously partitioned, where these are referred to as eluents that are eluted off of the column. Collection of the eluents was done using 20 mL scintillation vials.

An example of a fully packed column with its collection vial can be seen in Figure 5. This example photo was taken while U and Np were eluted from the column which explains the collection vial volume.

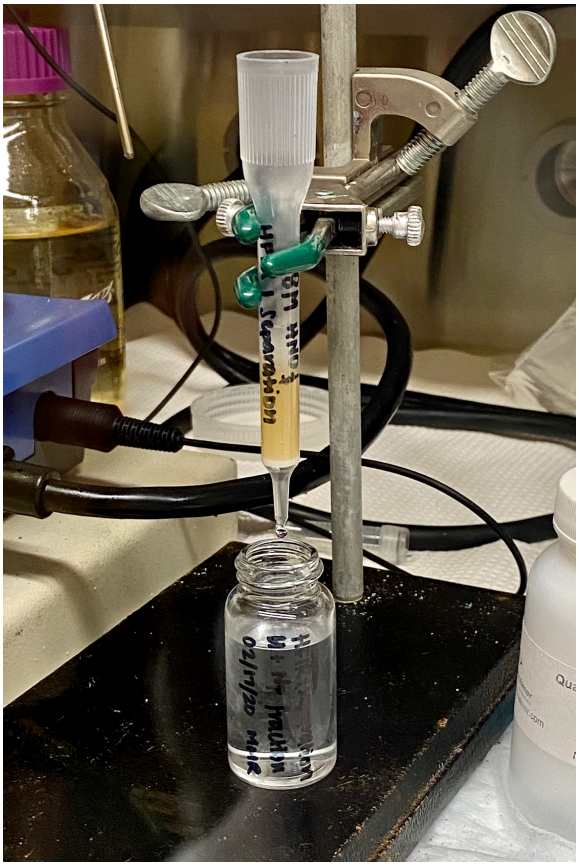

Figure 5. A fully packed column with its collection vial.

An approach to track the efficiency of a separation performed, while also adding detectable amounts of neptunium to a sample, is to spike a sample with ^{239}Np. Neptunium-239 was selected due to its strong gamma rays at energies 106.125(2), 277.599(1), and 228.183(1) keV. These peaks also do not overlap with X-rays and background peaks present in the laboratory setting. The initial approach to this problem was to construct an ^{243}Am – ^{239}Np generator. Once completed, this generator would provide an "endless" supply of neptunium every two weeks when secular equilibrium is achieved and can be used to spike the HFIR and MURR uranium samples with the generated ^{239}Np. [3] Once secular equilibrium is achieved the column can be milked for the ^{239}Np tracer and used to track the efficiency of an experiment and to determine whether activity was lost in a given destructive process. For the purpose of these experiments, and due to the non-completion of the ^{243}Am – ^{239}Np generator, 0.1 % of the ^{243}Am – ^{239}Np supply was added to the HFIR and MURR samples. Therefore, when HFIR and MURR are mentioned for radiochemical separation and analysis it is noted that these samples are spiked.

The resin used throughout this separation was DOWEX 1 x 8, 100 – 200 mesh size with a 1 mL resin bed. This resin was chosen due to its affinity for Pu in 8 M HNO_3. This acid concentration was chosen due to its ability to elute the uranium(VI), neptunium(V), americium(III) and fission products from the plutonium present in the HFIR and MURR sample. [31] The HFIR and MURR samples were initially dissolved in 1 mL of 8 M HNO_3 and loaded onto the head of the designated column.

Three different volumes, of a total volume of 2 mL, were used to ensure all of the irradiated sample was added to the head of the column during a quantitative transfer. This means the loading solution was 3 mL in total volume. Fifteen bed volumes (15 mL) of 8 M HNO_3 were used to elute U(VI), Np(V), Am and fission products from the Pu. The separated uranium nitrate,

neptunium nitrate, americium nitrate and fission products can be seen in Figure 5 for one of the HFIR samples. This process was repeated three separate times for both HFIR and MURR resulting in six separate vials of 18 mL each. All of the plutonium remained on the column and eluted with 0.01 M HNO_3. A lower concentration of HNO_3 was selected due the low affinity to the DOWEX 1 x 8 resin at this concentration. [31, 32] Sixty bed volumes (60 mL) were used to recover the Pu from the column, as seen in Figure 6.

Figure 6. Collection of Pu from the HNO_3 column using 0.01 M HNO_3.

The 18 mL of uranium nitrate, neptunium nitrate, americium nitrate and fission products solution were evaporated to dryness. This step was continued until all nitric acid evaporated. A surrogate sample of just 8 M HNO_3 was made to evaporate simultaneously with the ‘U & Np

fraction' sample. The purpose of the surrogate sample was to perform the next steps of radiochemistry prior to performing the next steps on the radioactive sample to prevent destruction of the sample. Once the HNO_3 was evaporated at 110°C, the U, Np, Am, and fission products remained in the scintillation vial. The contents of this vial were dissolved in 6 M HCl and evaporated to dryness. This step was repeated three times, and the same precautions were taken for the surrogate vial, after evaporation, the samples were dissolved in 2% HNO_3 to be further analyzed with ICP-MS.

2.1.2 Single Column Extraction Chromotographic Separation of HFIR Material

The following procedure was followed to achieve separation of the HFIR material. Figure 7 outlines the procedure used for single column chromatography. [11] This system was modeled after a similar separation scheme by A. Morgenstern *et al.* [16] It is worth noting that this method was different than previously mentioned; in this instance the flow rate was controlled by injecting the mobile phase with a syringe.

HFIR material was loaded onto a cartridge of UTEVA resin within the glovebox, along with 6 M HNO_3 and 0.3% of H_2O_2. Various rinse stages were utilized to elute the nuclide of interest at a given step. The rinse stages used altered a nuclide's affinity for the resin by changing the complexation of the nuclide of interest. To elute Am(III), Ln(III), and fission products from the column, a rinse state of 6 M HNO_3 and 0.3 % of H_2O_2 was pushed through the column with a syringe. Rinse stage two consisted of 2 M HNO_3, 2×10^{-3} M ascorbic acid, 2×10^{-3} M NH_2OH to elute Pu(III) from the column. Next, Np(IV) was eluted from the column using 2 M HNO_3 and 0.1 M oxalic acid. Lastly, U(VI) was eluted from the column using 7×10^{-3} M $(NH_4)_2C_2O_4$. The separated samples were individually removed from the glovebox, checked for contamination, and properly handled before being transported to the high purity germanium

detector for preliminary counting. This scheme would not work on the MURR sample due to the small quantities of neptunium in the sample so analysis was done using ICP-MS. These separated samples were analyzed using gamma spectroscopy to verify that full separation occurred.

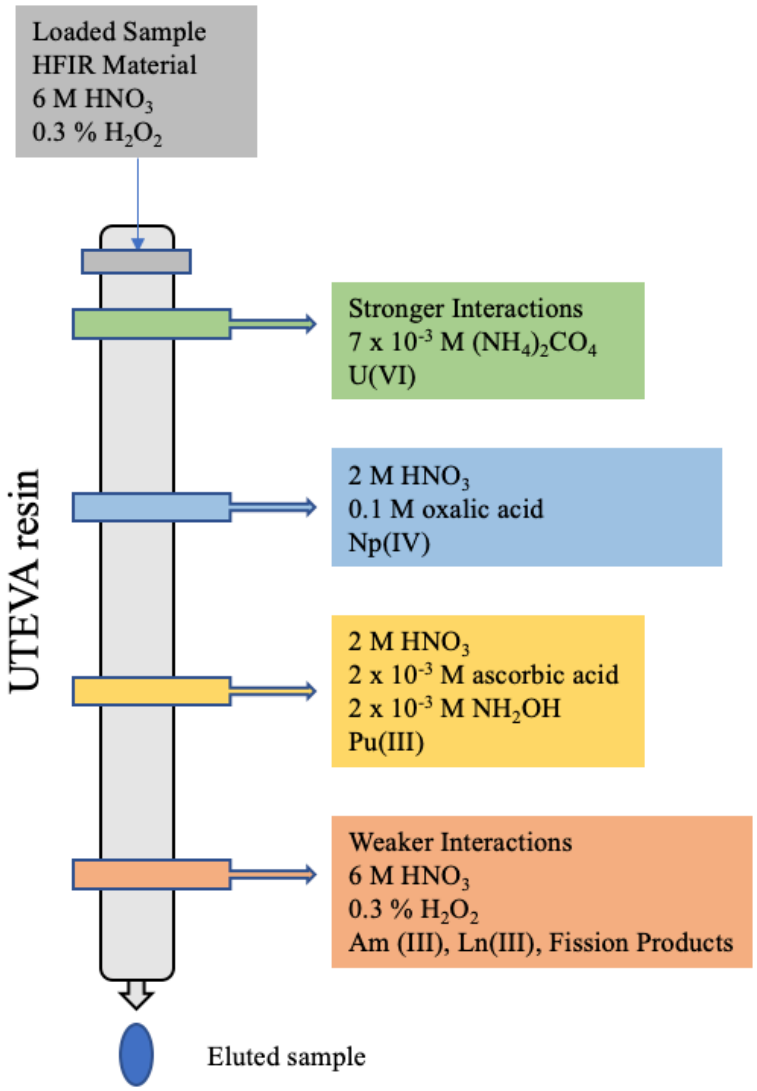

Figure 7. Single Column Extraction Chromatographic Separation of HFIR material, [11] isolation of neptunium from HFIR.

2.2 Preparation of ICP-MS Standards and Samples

In order to accurately quantify the small concentration of neptunium and uranium in a sample, standards had to be made to calibrate the ICP-MS. The standards made were of 100 parts per billion (ppb), 10 ppb, 1 ppb, 0.1 ppb, and 0.01 ppb in 2% nitric acid. Parts per billion is defined as nanograms per milliliter (ng ml^{-1}). This was accomplished using serial dilution where a small sample from the prior ppb mixture was used to make the next lower concentration in ppb. Next, the radioactive samples needed to be measured using gamma spectroscopy to estimate how much uranium exists within a sample. This estimation was accomplished by measuring the ^{137}Cs gamma peak, 662 keV, to determine the fraction of the pellet that was in a given sample. It is assumed that the amount of ^{137}Cs in a sample is proportional to the uranium content in the pellet.

A sample was placed on the high-purity germanium detector (HPGe) and counted for approximately 2,000 s. This length of time was chosen because it gave sufficient counting statistics to be used to approximate the fraction of the pellet present in a given sample. This is done because the fraction of the pellet can be used to determine the amount of U in a aliquot of a given size. The values used throughout the calculations in Eqs. 8-14 can be found in Table 2.

Table 2. Constants needed to perform calculations listed out in Eq. 8 - Eq. 14.

Date of Experiment	10/9/20
Elapsed Time (d)	2596
Elapsed Time (yr)	7.017
Number of Pellets (HFIR)	6
Number of Pellets (MURR)	3
The mass of U in HFIR pellet (g)	1.14E-02
The mass of U in MURR pellet (g)	1.29E-02
Desired mass of Np	1.00E-09
Avogadro's Number	6.02E+23
Efficiency of HPGe for 662.1 keV	0.45 %
Yield for ^{137}Cs	0.85

A region of interest was set on the 661.7 keV gamma peak and analyzed on each sample to obtain the number of counts and the associated error in the peak. The net count rate was used to determine the activity of ^{137}Cs in Eq. 8.

$$Activity\ (Bq) = \frac{Net\ Count\ Rate\ (s^{-1})}{Yield\ x\ Efficiency} \quad \text{Eq. 8}$$

The mass (g), shown in Eq. 9, was determined using the activity (Bq), the molar mass of ^{137}Cs, 136.907 g/mol, and the decay constant where ^{137}Cs has a half-life of 30.08 years, shown in Eq. 10.

$$Mass\ (g) = \frac{Activity\ (Bq)\ x\ Molar\ Mass\ (\frac{g}{mol})}{Decay\ Constant\ (s^{-1})\ x\ Avagadro's\ Number(mol^{-1})} \quad \text{Eq. 9}$$

$$\lambda = \frac{\ln(2)}{T_{1/2}} \quad \text{Eq. 10}$$

Measuring the fraction of the pellet used is important to determine the amount of U and Np present in an aliquot of a given volume. The fraction of the pellet was determined using the mass obtained using Eq. 9 and Eq. 11.

$$Fraction\ of\ Pellet = \frac{Mass\ (g)}{Mass\ present\ in\ sample\ at\ time, T} \quad \text{Eq. 11}$$

The amount of U present in an aliquot utilizes the calculated fraction of the pellet and using Eq. 12. This equation determines how much U is present in a sample of that size and it is important to make samples that are 1 ppb while the Np present in the aliquot is 10 ppb. The amount of Np present in the aliquot was determined using Eq. 13.

$$U\ in\ aliquot\ (g) = Fraction\ of\ Pellet\ x\ the\ total\ mass\ of\ U\ in\ a\ sample\ (g) \quad \text{Eq. 12}$$

$$Np\ in\ aliquot\ (g) = U\ in\ aliquot\ (g)\ x\ fraction\ of\ Np\ in\ spent\ fuel \quad \text{Eq. 13}$$

The amount of Np present in an aliquot was then used to determine the concentration of Np present in a sample and then multiplied by the estimated fraction of Np in spent fuel, shown in Eq. 14. The amount of neptunium produced is approximately 0.1% of the mass of uranium but this value is at intended discharge burnup. However, for the HFIR and MURR samples which were irradiated and taken from the reactor at low burnup an assumption was made that approximately 0.01% of Np was produced, this result was later determined to be lower per simulation data.

$$Concentration\ in\ (g/mL) = \frac{Np\ in\ aliquot\ (g)}{Volume\ of\ aliquot\ (mL)} \quad \text{Eq. 14}$$

This series of calculations was done for unaltered MURR and HFIR samples as well as separated samples where the Pu content was extracted using column chromatography. The standards and ICP-MS samples can be seen below in Figures 8-10.

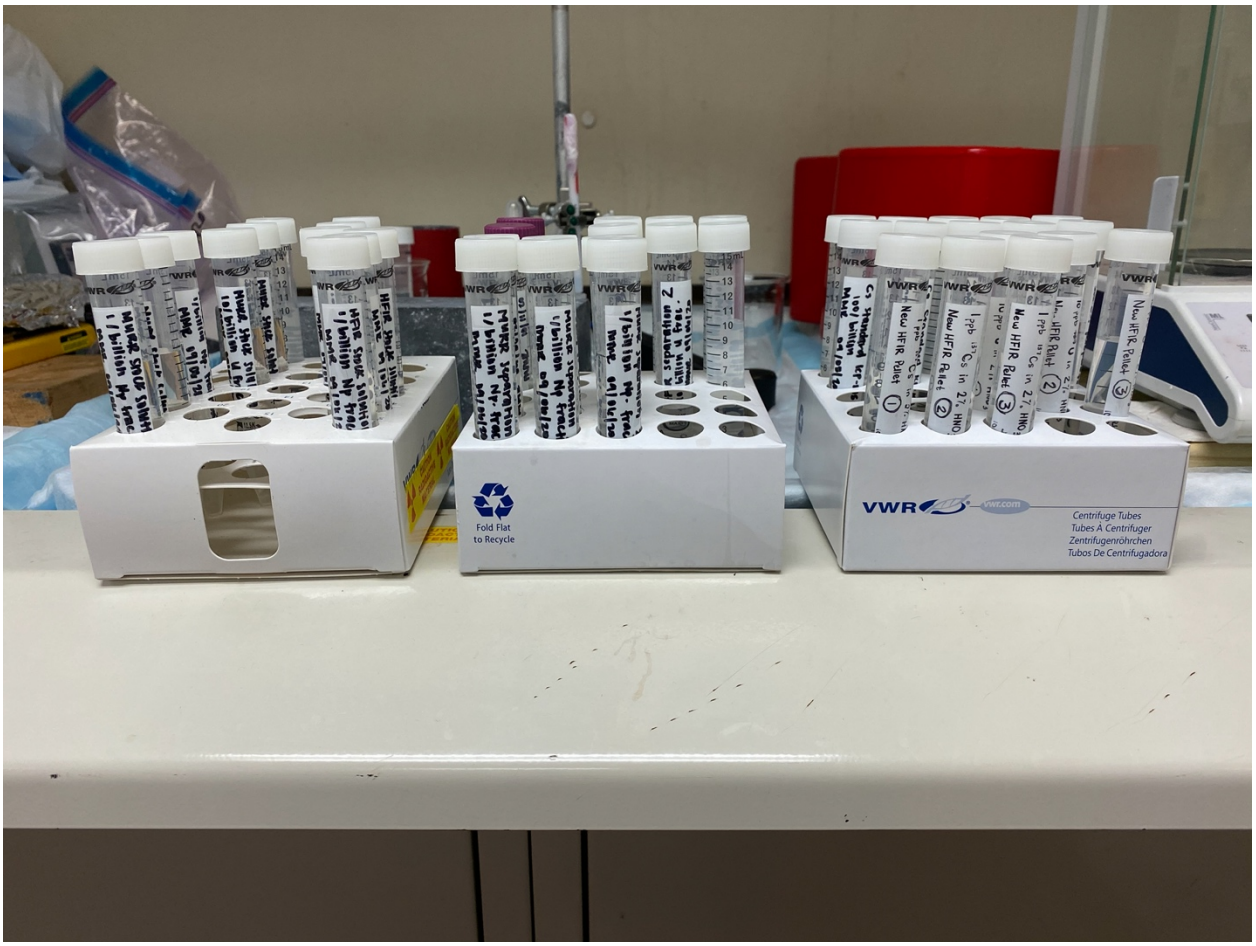

Figure 8. Completed samples for HFIR and MURR samples along with samples that underwent column chromatography and standards awaiting ICP-MS.

Figure 9. HFIR and MURR stock solution samples that are prepared for 1 ppb for Np observation and 10 ppb for U.

Figure 10. HFIR and MURR samples that underwent single column chromatography prepared for 1 ppb for Np observation and 10 ppb for U.

2.3 ORIGEN2.0 Fuel Modeling

Given the unique irradiated uranium samples that TAMU has access to, it was important to preform radiochemical analysis on these samples to quantify how much ^{237}Np was produced during the irradiation periods. However, due to irregular irradiation patterns and unknown displacement of the irradiated material at HFIR the sample was not comparable to an FBR irradiation. One way to quantify the ^{237}Np production for commonly used rectors is to simulate the fuel burn-up using *ORIGEN2.0* for PWR, BWR, CANDU, and FBR. These simulations were modeled to irradiate one-metric-ton of fuel to full and low burnup to monitor Np production so the data could be comparable to the HFIR and MURR irradiations. HFIR and MURR irradiations were modeled in *MCNPX* and *MCNP*®6 and used in comparison to *ORIGEN2.0* simulations.

ORIGEN2.0 calculates build-up, burn-up, decay, and depletion of radioactive materials. This is useful for simplified fuel modeling compared to *MCNP*®6 calculations which requires geometry and specifications for fuel irradiation simulations. *ORIGEN2.0* models utilize built-in libraries for various reactor types. These libraries contain cross-section libraries that differ amongst reactor types. Decay libraries are utilized as well for further analysis of nuclear material; within these there are separate libraries for cross section information and yield factors for activation products, actinides, and fission products. This is of importance when modeling spent nuclear fuel and how the actinides, minor actinides, and fission products change over time.

3. RESULTS

3.1 Fuel Enrichment and Specifications

Four separate reactors were modeled in ORIGEN2.0 using the appropriate specifications indicated in the ORIGEN2.0 manual and literature. The cross-section libraries utilized are found in Table 3 for each reactor type. The number of days it took to achieve the intended discharge burnup of the modeled fuel for each of the reactor types can be found in Table 4. The decay libraries, or cross-section libraries found in Table 3, are split into three separate category of isotopes: activation products, actinides, and fission products, respectively. An example input for full and low burnups can be found in Appendix A and B for a PWRUS input.

Table 3. Cross-section libraries and corresponding variable cross-section libraries for the various reactor types modeled: pressurized water reactor (PWR), boiling water reactor (BWR), Canada deuterium uranium reactor (CANDU), and fast breeder reactor (FBR) with the associated specific power.

Reactor Type	Cross-Section Libraries			Variable Cross-Section Data	Specific Power (W/g)
	Activation Product	Actinide	Fission Product		
PWRU	204	205	206	1	37.5
PWRUS	601	602	603	38	37.5
BWRU	251	252	253	4	25.9
BWRUS	651	652	653	40	25.9
CANDU	401	402	403	21	16.5
FBR	311	312	313	12	116

Table 4. Number of days it took for the PWR, BWR, CANDU, and FBR to reach full burnup and low burnup. *Decay present for 106.0 days every three burn steps.

Reactor Type	Number of days to achieve full burnup	Full Burnup (MWd/MT)	Number of days to achieve low burnup	Low Burnup (MWd/MT)
PWRU	1200.0	45,000	133.33	5,000
PWRUS	1200.0	45,000	133.33	5,000
BWRU	1862.4*	40,000	193.05	5,000
BWRUS	1862.4*	40,000	193.05	5,000
CANDU	454.54	7,500	303.03	5,000
FBR	689.65	80,000	43.1	5,000

The number of days a specific reactor took to achieve the intended discharged burnup is directly correlated to the specific power, in units of W/g, amount of fuel, in units of grams, and the fuel enrichment, in units of atom percent. The correlation can be defined by Eq. 15, which shows the relationship between burnup calculations and the specifications. For the purposes of this study all reactors were modeled using one metric tonne of the typical fuel and enrichment for a given reactor. The fuel enrichment and compositions can be found in Table 5 below.

$$Burnup\ (MWd/MT) = \frac{Specific\ Power\ \left(\frac{W}{g}\right)\ x\ Time\ (d)}{one\ metric\ tonne\ of\ fuel\ (g)} \quad \text{Eq. 15}$$

The proper way to annotate nuclides for *ORIGEN2.0* is in Eq. 16, where Z is the atomic number of the nuclide, A is the atomic mass, and IS is the isomeric state which is either ground or excited. When a nuclide is in its ground state it is represented by a 0 and when it is in an excited state it is represented as a 1. As an example using Eq. 16, ^{235}U would be written as 922350.

$$Nuclide\ of\ Interest = 1000\ x\ Z + 10A + IS \quad \text{Eq. 16}$$

Table 5. Fuel enrichment given in units of atom percent and fuel composition (as written in *ORIGEN2.0*) for the corresponding nuclear reactor.

Reactor Type	Fuel Composition (Nuclide of Interest and g)	Fuel Enrichment (%)
PWRU	922340 270. 922350 30000. 922380 969730. 80160 1186.	3.0
PWRUS	922340 270. 922350 30000. 922380 969730. 80160 1186.	3.0
BWRU	922340 270. 922350 41000. 922380 958730. 80160 1186.	4.31
BWRUS	922340 270. 922350 41000. 922380 958730. 80160 1186.	4.31
CANDU	922340 50. 922350 7110. 922380 992840. 80160 1186.	^{nat}U
FBR	922350 1444.8 922380 933354. 942380 50.100 80160 1186. 942390 15228.1 942400 40408.4 942410 7050.29 942420 2464.5	^{dep}U

3.2 ORIGEN2.0 Fuel Burn-up Determination

Typically the amount of ^{237}Np produced is low but over several tonnes, years of operation, and decay the total amount increases from the beta decay of ^{237}U and the alpha decay of ^{241}Am. The half-life of ^{237}U is 6.75 days which leads to increases in the amount of ^{237}Np present in spent fuel to increase within 10 half-lives of ^{237}U. The half-life of ^{241}Am is 432 years which leads to increases in the amount of ^{237}Np present in stored, used nuclear fuel in the long term.

Following the specifications laid out in Tables 3-5, in section 3.1, the following data were obtained for the various reactors. The tables provide the production, in units of grams, for each nuclide produced in the given timeframe and how the nuclide production varied with decay. The reactor fuel was modeled to discharge the spent fuel at full intended burnup in Tables 6-10. These tables were used to validate the production rate for ^{237}Np while Table 11 and Table 12 were used to validate the total Pu production in the *ORIGEN2.0* reactor models.

Table 6. Production of nuclide buildup in a BWRUS at a burnup of 40,000 MWd/MTU.

BWRUS | Production (g) of Nuclides					
Number of days (d)	1862.4	1962.4	3057.4	3787.4	5612.4
Burnup (MWd/MT)	40,000	100 day decay	3 year decay	5 year decay	10 year decay
^{237}Np	6.51E+02	6.63E+02	6.63E+02	6.64E+02	6.68E+02
^{237}U	1.12E+01	4.27E-04	3.31E-05	3.01E-05	2.37E-05
^{241}Am	5.81E+01	7.45E+01	2.40E+02	3.37E+02	5.42E+02

Table 7. Production of nuclide buildup in a BWRU at a burnup of 40,000 MWd/MTU.

BWRU | Production (g) of Nuclides					
Number of days (d)	1862.4	1962.4	3057.4	3787.4	5612.4
Burnup (MWd/MT)	40,000	100 day decay	3 year decay	5 year decay	10 year decay
^{237}Np	5.85E+02	5.95E+02	5.95E+02	5.96E+02	6.00E+02
^{237}U	9.65E+00	3.74E-04	3.36E-05	3.05E-05	2.40E-05
^{241}Am	5.23E+01	6.90E+01	2.37E+02	3.35E+02	5.43E+02

Using the BWRUS/ BWRU cross-section libraries, a specific power of 25.9 W/g, and an average fuel enrichment of 4.31 w/o, it took approximately 1862.4 days to achieve a full burnup of 40,000 MWd/MT. This produced 6.51E+02 g and 5.85E+02 g of ^{237}Np per tonne of fuel, respectively.

Table 8. Production of nuclide buildup in a PWRUS at a burnup of 45,000 MWd/MTU.

PWRUS | Production (g) of Nuclides					
Number of days (d)	1200.0	1300.0	2395.0	3125.0	4950.0
Burnup (MWd/MT)	45,000	100 day decay	3 year decay	5 year decay	10 year decay
^{237}Np	6.73E+02	6.88E+02	6.89E+02	6.90E+02	6.94E+02
^{237}U	1.46E+01	5.54E-04	4.12E-05	3.74E-05	2.94E-05
^{241}Am	4.34E+01	6.38E+01	2.70E+02	3.91E+02	6.45E+02

Table 9. Production of nuclide buildup in a PWRU at a burnup of 45,000 MWd/MTU.

PWRU | Production (g) of Nuclides					
Number of days (d)	1200.0	1300.0	2395.0	3125.0	4950.0
Burnup (MWd/MT)	45,000	100 day decay	3 year decay	5 year decay	10 year decay
^{237}Np	6.21E+02	6.34E+02	6.35E+02	6.36E+02	6.41E+02
^{237}U	1.29E+01	4.96E-04	4.33E-05	3.93E-05	3.09E-05
^{241}Am	4.06E+01	6.20E+01	2.78E+02	4.06E+02	6.73E+02

Using the PWRUS/ PWRU cross-section libraries, a specific power of 37.5 W/g, and an average fuel enrichment of 3.0 w/o, it took 1200 days to achieve a full burnup of 45,000 MWd/MT. This produced 6.73E+02 g and 6.21E+02 g of ^{237}Np per tonne of fuel, respectively.

Table 10. Production of nuclide buildup in a CANDU at a burnup of 7,500 MWd/MTU.

CANDU | Production (g) of Nuclides					
Number of days (d)	454.5	554.5	1649.5	2379.5	4204.5
Burnup (MWd/MT)	7,500	100 day decay	3 year decay	5 year decay	10 year decay
^{237}Np	2.68E+01	2.77E+01	2.78E+01	2.79E+01	2.85E+01
^{237}U	9.32E-01	3.88E-05	5.56E-06	5.05E-06	3.97E-06
^{241}Am	3.16E+00	5.91E+00	3.37E+01	5.01E+01	8.44E+01

Using the CANDU cross-section libraries, a specific power of 16.5 W/g, and an natural uranium as the fuel source, it took 454.5 days to achieve a full burnup of 7,500 MWd/MT. This produced 2.68E+01 g of ^{237}Np per tonne of fuel.

In Tables 6-10 the masses of ^{237}U and ^{241}Am were listed for decay analysis since it was observed that the production of ^{237}Np increased as time passed. This was due to the decay of ^{237}U because of its relatively short half-life in comparison to ^{241}Am long half-life. This was verified by adding the starting production of ^{237}U and to ^{237}Np and calculating the discrepancy between the ending and beginning quantity. This concluded that the ^{237}U was contributing to the overall ending amount. The assumption is that there are trace amounts of ^{237}U produced for a short time after full burnup is achieved; eventually the amount of ^{237}Np will increase as the ^{241}Am begins to alpha decay.

After intended discharge burnup is reached, the reactors were ranked according to their overall ^{237}Np production . Based on the results found in Tables 6-10, it was determined that a PWR produced the most ^{237}Np, respectively followed by BWR, CANDU, and FBR. Again, the contributing factors that affect production rates are the starting fuel enrichment and the specific power.

PWRs and BWRs produce the highest quantity of ^{237}Np due to higher fuel enrichment. This means the ^{235}U content is higher in PWRs and BWRs than it is in a CANDU reactor, which burns natural uranium, and FBRs, which burn depleted uranium. The differences in production between a PWR and BWR are due to the fuel pellet and rod size. The radius of the fuel is larger for a BWR than a PWR which creates a larger mean free path for neutrons. This results in a slightly less thermal spectrum for the reactor. The more thermal a reactor, the more neptunium is produced. Another key role in the neptunium production for these two reactors is that the

irradiation histories differ. When comparing a CANDU reactor to a FBR the CANDU operates with a more thermal spectrum that is comparable to a BWR and PWR, whereas a FBR has a fast spectrum. The spectra differences between the reactor types plays a contributing role because the ^{236}U neutron capture cross-section is higher in thermal regions.

As described in the introduction, ^{237}Np has a fast neutron fission cross-section comparable to that of ^{239}Pu, and its production rate is roughly 0.1% of used nuclear fuel whereas Pu makes up roughly 1%. To validate the results of this study the ^{237}Np production and total Pu production were determined. Tables 11 and 12 show the quantity of the Pu nuclides for the discharged fuel for a PWR, using the PWRUS libraries, and a CANDU reactor. The total Pu content for the PWRUS model was 1.13E+04 g per one metric tonne of fuel. This results in the Pu content as 1% of the fuel which agrees with literature. The amount of ^{237}Np attributed to approximately 0.06% of the total spent fuel; however, not all neptunium nuclides were included in the approximation due to short half-life and non-weapon use suspicions. Nonetheless, the ^{237}Np makes up approximately 0.1% of the spent fuel which agrees with literature. These results allow for the conclusion to be made that the *ORIGEN2.0* reactor models were valid in their determination of the overall production of ^{237}Np.

Table 11. Production of nuclide buildup in a PWR at a burnup of 45,000 MWd/MTU.

PWRUS | Production (g) of Nuclides					
Number of days (d)	1200.0	1300.0	2395.0	3125.0	4950.0
Burnup (MWd/MT)	45,000	100 day decay	3 year decay	5 year decay	10 year decay
^{236}Pu	1.88E-03	1.77E-03	8.51E-04	5.24E-04	1.55E-04
^{237}Pu	4.10E-04	8.96E-05	5.30E-12	8.03E-17	7.19E-29
^{238}Pu	2.96E+02	3.04E+02	3.09E+02	3.05E+02	2.93E+02
^{239}Pu	5.63E+03	5.74E+03	5.74E+03	5.74E+03	5.74E+03
^{240}Pu	2.93E+03	2.93E+03	2.95E+03	2.95E+03	2.97E+03
^{241}Pu	1.56E+03	1.54E+03	1.33E+03	1.21E+03	9.51E+02
^{242}Pu	8.70E+02	8.70E+02	8.70E+02	8.70E+02	8.70E+02
^{243}Pu	3.14E-01	5.89E-13	5.89E-13	5.89E-13	5.89E-13
^{244}Pu	1.13E-01	1.13E-01	1.13E-01	1.13E-01	1.13E-01
^{245}Pu	3.20E-06	0.00E+00	0.00E+00	0.00E+00	0.00E+00
^{246}Pu	3.10E-08	5.21E-11	6.39E-18	6.39E-18	6.38E-18

Table 12. Production of nuclide buildup in a CANDU at a burnup of 7,500 MWd/MTU.

CANDU | Production (g) of Nuclides					
Number of days (d)	454.5	554.5	1649.5	2379.5	4204.5
Burnup (MWd/MT)	7,500	100 day decay	3 year decay	5 year decay	10 year decay
^{236}Pu	3.11E-06	2.94E-06	1.42E-06	8.73E-07	2.59E-07
^{237}Pu	1.16E-06	2.54E-07	1.50E-14	2.28E-19	2.04E-31
^{238}Pu	3.46E+00	3.74E+00	4.06E+00	4.00E+00	3.84E+00
^{239}Pu	2.72E+03	2.77E+03	2.77E+03	2.77E+03	2.77E+03
^{240}Pu	1.04E+03	1.04E+03	1.04E+03	1.04E+03	1.04E+03
^{241}Pu	2.10E+02	2.08E+02	1.80E+02	1.63E+02	1.28E+02
^{242}Pu	5.26E+01	5.26E+01	5.26E+01	5.26E+01	5.26E+01
^{243}Pu	5.27E-03	1.39E-17	1.39E-17	1.39E-17	1.39E-17
^{244}Pu	4.75E-04	4.75E-04	4.75E-04	4.75E-04	4.75E-04
^{245}Pu	1.23E-08	0.00E+00	0.00E+00	0.00E+00	0.00E+00
^{246}Pu	1.07E-10	1.80E-13	7.40E-24	7.40E-24	7.40E-24

3.2.1 ORIGEN2.0 Low Burnup Determination

TAMU has two uniquely irradiated uranium samples from HFIR and MURR. These two pellets were analyzed using ICP-MS to quantify how much ^{237}Np was present in each sample. However, the *MCNP*®6 models previously developed and published [22-27, 33] were used to compare the simulated production levels of ^{237}Np to the *ORIGEN2.0* simulation at the same low burnup of 5,000 MWd/MT. The data from the *MCNP*®6 models for HFIR and MURR can be found in Table 13. It is worth noting that the amount of neptunium produced in the *MCNP*®6 simulations was representative of the production rate of the irradiated pellets, not MURR or HFIR fuel as a whole.

The mass of U in the HFIR pellet was 1.14E-02 g and the mass present in the MURR pellet was 1.29E-02 g. There were 6 total HFIR pellets and 3 total MURR pellets. The samples used for analysis were measured using a HPGe detector. The ^{137}Cs peak information was used to make a comparison of the amount of uranium present in a sample and divided by the total number of pellets. At time of *T*, a single HFIR pellet contained 2.18E-06 g of ^{137}Cs while a single MURR pellet had 1.57E-07 g of ^{137}Cs. This value was assumed to be equivalent to the ^{235}U content for the pellet.

Table 13. Mass of ^{237}Np, ^{238}Np, and ^{239}Np present in a given reactor type for a determined power-level, over a span of time.

Reactor Type	Burn-up (GWd/MTU)	Quantity of Actinide Present (g)		
		^{237}Np	^{238}Np	^{239}Np
HFIR	4.965E+00	2.079E-06	6.220E-08	1.681E-04
	1.352E+00	1.911E-06	4.727E-08	1.477E-04
MURR	4.363E+00	2.304E-07	7.172E-10	6.238E-06
	2.359E+00	3.690E-08	1.296E-10	4.154E-06

The values presented in Table 13 were used to normalize the information presented in Table 14. In order to perform the normalizations, the amount of ^{237}Np present in the six HFIR

pellets and three MURR pellets were converted from mass, in units of grams, per pellet to the amount produced in one tonne of fuel.

Table 14. Mass of ^{237}Np produced in HFIR and MURR per irradiated pellet and per tonne of fuel.

Reactor Type	Burn-up (GWd/MTU)	^{237}Np (g) per pellet	^{237}Np (g) for one metric tonne
HFIR	4.965E+00	3.47E-07	3.47E-01
	1.352E+00	3.19E-07	3.19E-01
MURR	4.363E+00	7.68E-08	7.68E-02
	2.359E+00	1.23E-08	1.23E-02

Following the specifications laid out in Tables 3-5 the following data was obtained for the various reactors, discharging spent fuel at a burnup of 5,000 MWd/MT in Tables 15-19. The number of days to complete the burn steps can be found in the tables for a given reactor. This was modeled for low burnup of one metric tonne of fuel following the same specifications listed in Tables 3-5 in Section 3.1. As mentioned in Section 3.2, the same ranking system is applicable at low burnups as in high burnups. The PWR produced the most ^{237}Np, followed by a BWR, and CANDU. The final column in Table 14 shows that HFIR and MURR, once extrapolated to one metric tonne of fuel, produced low quantities of ^{237}Np. This is due to the irradiation history for the pellet irradiations and low burnup.

Table 15. Production of nuclide buildup in a BWRUS at a burnup up to 5,000 MWd/MTU.

BWRUS | Production (g) of Nuclides					
Number of days (d)	38.6	77.2	115.8	154.4	193.1
Burnup (MWd/MT)	1000	2000	3000	4000	5000
^{237}Np	2.03E+00	1.03E+01	2.96E+01	6.69E+01	1.30E+02
^{237}U	7.67E-01	1.37E+00	2.11E+00	3.07E+00	4.23E+00
^{241}Am	4.41E-04	3.09E-02	3.99E-01	2.30E+00	8.10E+00

Table 16. Production of nuclide buildup in a BWRU at a burnup up to 5,000 MWd/MTU.

BWRU | Production (g) of Nuclides					
Number of days (d)	38.6	77.2	115.8	154.4	193.1
Burnup (MWd/MT)	1000	2000	3000	4000	5000
^{237}Np	1.72E+00	8.79E+00	2.57E+01	5.88E+01	1.16E+02
^{237}U	6.51E-01	1.18E+00	1.84E+00	2.70E+00	3.78E+00
^{241}Am	3.02E-04	2.15E-02	2.87E-01	1.73E+00	6.37E+00

Table 17. Production of nuclide buildup in a PWRUS at a burnup up to 5,000 MWd/MTU.

PWRUS | Production (g) of Nuclides					
Number of days (d)	26.7	53.3	80.0	106.7	133.3
Burnup (MWd/MT)	1000	2000	3000	4000	5000
^{237}Np	2.36E+00	6.69E+00	1.21E+01	1.85E+01	2.57E+01
^{237}U	1.36E+00	1.85E+00	2.26E+00	2.65E+00	3.02E+00
^{241}Am	5.49E-04	7.92E-03	3.68E-02	1.07E-01	2.38E-01

Table 18. Production of nuclide buildup in a PWRU at a burnup up to 5,000 MWd/MTU.

PWRU | Production (g) of Nuclides					
Number of days (d)	26.7	53.3	80.0	106.7	133.3
Burnup (MWd/MT)	1000	2000	3000	4000	5000
^{237}Np	2.74E+00	7.57E+00	1.34E+01	2.02E+01	2.77E+01
^{237}U	1.55E+00	2.03E+00	2.42E+00	2.79E+00	3.14E+00
^{241}Am	4.81E-04	6.91E-03	3.21E-02	9.30E-02	2.08E-01

Table 19. Production of nuclide buildup in a CANDU at a burnup up to 5,000 MWd/MTU.

CANDU | Production (g) of Nuclides					
Number of days (d)	60.6	121.2	181.8	242.4	303.0
Burnup (MWd/MT)	1000	2000	3000	4000	5000
^{237}Np	1.98E+00	4.86E+00	8.18E+00	1.19E+01	1.58E+01
^{237}U	4.33E-01	5.38E-01	6.28E-01	7.06E-01	7.80E-01
^{241}Am	4.53E-03	5.69E-02	2.27E-01	5.56E-01	1.07E+00

3.3 ICP-MS Sample Results

ICP-MS was used to analyze the aliquots of the HFIR and MURR standard samples due to its higher sensitivity for actinides in low concentrations compared to methods like gamma spectroscopy. In order to get the proper dilutions made for ICP-MS some assumptions had to be made in order to get sufficient estimations in ppb and ppm. Table 20 shows an estimated mass of uranium and neptunium present in a sample of a given aliquot size. These assumptions were made using the ^{137}Cs gamma peak, 662 keV, to determine the fraction of the pellet present. It was also assumed that the amount of ^{137}Cs in a sample is proportional to the uranium content in the pellet.

Based on literature, the amount of neptunium produced is approximately 0.1% of the total mass of uranium, however this value is at full burnup. For example, the intended discharge burnup is 45,000 MWd/MTU for a PWR and 40,000 MWd/MTU for a BWR, respectively. At lower burnups this approximation is expected to be smaller due to a lower number of days in the reactor. For the HFIR and MURR samples, which were irradiated and taken from the reactor at low burnup, an assumption was made that approximately 0.01% of the total mass was Np when preparing the samples. This assumption was made because the burnup for HFIR and MURR irradiations was approximately ten times lower than the full, high-burnup. The full intended burnup for a CANDU and FBR, whose irradiation histories were emulated by the MURR and HFIR irradiations, were 7,500 MWd/MTU and 80,000 MTd/MTU, respectively.

In order to analyze the ICP-MS raw data, a calibration curve needed was made using the data from the standards. This was done by observing the amount of counts per second (the Y-axis values) compared to concentrations (the x-axis values) of the solution at 100 ppb, 10 ppb 1 ppb, 0.1 ppb, and 0.01 ppb in 2% nitric acid. Again, parts per billion is defined as nanograms per milliliter (ng ml^{-1}).

Table 20. Estimated amounts of U and ^{237}Np present in a given aliquot size in ppb.

Volume (mL)	Identification	fraction of pellet (uL)	U in aliquot (g)	Np in aliquot (g)	concentration in g/mL	Np in ppb if 0.1% of total mass	Np in ppb if 0.01% of total mass
0.054	HFIR Stock Solution 1	0.64%	7.32E-05	7.32E-08	1.35E-06	1.35E+03	1.35E+02
0.054	HFIR Stock Solution 2	0.62%	7.02E-05	7.02E-08	1.30E-06	1.30E+03	1.30E+02
0.054	HFIR Stock Solution 3	0.41%	4.61E-05	4.61E-08	8.53E-07	8.53E+02	8.53E+01
0.03	MURR Stock Solution 1	0.16%	2.05E-05	2.05E-08	6.84E-07	6.84E+02	6.84E+01
0.03	MURR Stock Solution 2	0.16%	2.07E-05	2.07E-08	6.89E-07	6.89E+02	6.89E+01
0.03	MURR Stock Solution 3	0.16%	2.07E-05	2.07E-08	6.89E-07	6.89E+02	6.89E+01
0.1	HFIR Sep. Solution 1	0.03%	3.24E-06	3.24E-09	3.24E-08	3.24E+01	3.24E+00
0.1	HFIR Sep. Solution 2	0.09%	1.06E-05	1.06E-08	1.06E-07	1.06E+02	1.06E+01
0.1	HFIR Sep. Solution 3	0.12%	1.38E-05	1.38E-08	1.38E-07	1.38E+02	1.38E+01
0.1	MURR Sep. Solution 1	0.00%	-5.02E-10	-5.02E-13	-5.02E-12	-5.02E-03	-5.02E-04
0.1	MURR Sep. Solution 2	0.10%	1.27E-05	1.27E-08	1.27E-07	1.27E+02	1.27E+01
0.1	MURR Sep. Solution 3	0.11%	1.39E-05	1.39E-08	1.39E-07	1.39E+02	1.39E+01

The concentration of the solutions for the uranium standards was multiplied by the isotopic abundance of ^{235}U and ^{238}U. The concentration was then converted to log-scale by taking the logarithmic value of the abundance corrected concentration in ppb. The counts per second recorded by the ICP-MS was then converted to log-scale. The purpose of using log-scale was to see the "linear" relationship between recorded count rate and concentration of solution. It is noteworthy that the best-fit line produced from the linear fit is a logarithmic value that needs to be converted during analysis. During data analysis, the uncertainty of the ^{235}U calibration caused substantial error. For this reason, the calibration curve for ^{235}U was not used and all data was normalized to the ^{238}U calibration curve. The calibration curve used for analysis can be seen in Figure 11. Tables 21-25 show the calculated concentration of ^{235}U, ^{238}U, ^{237}Np, ^{239}Pu, and ^{240}Pu in the samples. The HFIR aliquot size was 0.072 mL of the stock solution per sample and the MURR aliquot size was 0.024 mL of the stock solution per sample.

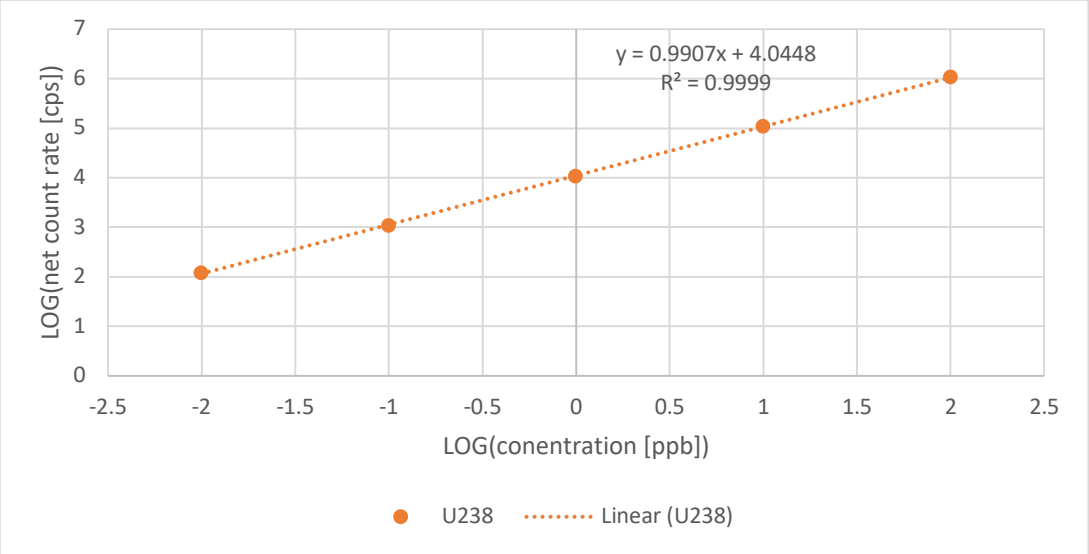

Figure 11. The calibration curve for ^{238}U with a linear fit trendline.

Table 21. The concentration of ^{235}U calculated using the best-fit line for the ^{238}U standard.

^{235}U					
Sample Name	X (ppb in log scale)	x (ppb)	x (g/mL)	x (g)	fraction
HFIR Stock 1 - Np	2.526	335.366	3.35E-07	2.41E-08	2.95E-03
HFIR Stock 2 - Np	2.509	322.677	3.23E-07	2.32E-08	2.84E-03
HFIR Stock 3 - Np	2.326	212.018	2.12E-07	1.53E-08	1.86E-03
HFIR Stock 1 - U	0.510	3.234	3.23E-09	2.33E-10	2.84E-05
HFIR Stock 2 - U	0.494	3.121	3.12E-09	2.25E-10	2.74E-05
HFIR Stock 3 - U	0.302	2.005	2.00E-09	1.44E-10	1.76E-05
MURR Stock 1 - Np	2.821	661.628	6.62E-07	1.59E-08	5.13E-03
MURR Stock 2 - Np	2.805	638.305	6.38E-07	1.53E-08	4.95E-03
MURR Stock 3 - Np	2.810	645.609	6.46E-07	1.55E-08	5.00E-03
MURR Stock 1 - U	0.823	6.658	6.66E-09	1.60E-10	5.16E-05
MURR Stock 2 - U	0.848	7.048	7.05E-09	1.69E-10	5.46E-05
MURR Stock 3 - U	0.826	6.703	6.70E-09	1.61E-10	5.20E-05

Table 22. The concentration of ^{238}U calculated using the best-fit line for the ^{238}U standard.

^{238}U					
Sample Name	X (ppb in log scale)	x (ppb)	x (g/mL)	x (g)	fraction
HFIR Stock 1 - Np	5.069	117312.749	1.17E-04	8.45E-06	1.03E+00
HFIR Stock 2 - Np	5.049	111827.901	1.12E-04	8.05E-06	9.83E-01
HFIR Stock 3 - Np	4.871	74263.594	7.43E-05	5.35E-06	6.53E-01
HFIR Stock 1 - U	3.043	1104.186	1.10E-06	7.95E-08	9.71E-03
HFIR Stock 2 - U	3.028	1066.034	1.07E-06	7.68E-08	9.37E-03
HFIR Stock 3 - U	2.837	686.744	6.87E-07	4.94E-08	6.04E-03
MURR Stock 1 - Np	5.046	111268.339	1.11E-04	2.67E-06	8.63E-01
MURR Stock 2 - Np	5.034	108110.154	1.08E-04	2.59E-06	8.38E-01
MURR Stock 3 - Np	5.035	108295.528	1.08E-04	2.60E-06	8.40E-01
MURR Stock 1 - U	3.013	1031.538	1.03E-06	2.48E-08	8.00E-03
MURR Stock 2 - U	3.034	1082.432	1.08E-06	2.60E-08	8.39E-03
MURR Stock 3 - U	3.027	1065.341	1.07E-06	2.56E-08	8.26E-03

Table 23. The concentration of ^{237}Np calculated using the best-fit line for the ^{238}U standard.

^{237}Np					
Sample Name	X (ppb in log scale)	x (ppb)	x (g/mL)	x (g)	fraction
HFIR Stock 1 - Np	0.635	4.314	4.31E-09	3.11E-10	3.79E-05
HFIR Stock 2 - Np	0.619	4.162	4.16E-09	3.00E-10	3.66E-05
HFIR Stock 3 - Np	0.436	2.730	2.73E-09	1.97E-10	2.40E-05
HFIR Stock 1 - U	-1.396	0.040	4.02E-11	2.89E-12	3.53E-07
HFIR Stock 2 - U	-1.418	0.038	3.82E-11	2.75E-12	3.35E-07
HFIR Stock 3 - U	-1.588	0.026	2.58E-11	1.86E-12	2.27E-07
MURR Stock 1 - Np	-0.802	0.158	1.58E-10	3.79E-12	1.22E-06
MURR Stock 2 - Np	-0.803	0.157	1.57E-10	3.78E-12	1.22E-06
MURR Stock 3 - Np	-0.792	0.161	1.61E-10	3.87E-12	1.25E-06
MURR Stock 1 - U	-2.841	0.001	1.44E-12	3.46E-14	1.12E-08
MURR Stock 2 - U	-2.663	0.002	2.17E-12	5.21E-14	1.68E-08
MURR Stock 3 - U	-2.728	0.002	1.87E-12	4.49E-14	1.45E-08

Table 24. The concentration of ^{239}Pu calculated using the best-fit line for the ^{238}U standard.

^{239}Pu					
Sample Name	X (ppb in log scale)	x (ppb)	x (g/mL)	x (g)	fraction
HFIR Stock 1 - Np	3.243	1749.136	1.75E-06	1.26E-07	1.54E-02
HFIR Stock 2 - Np	3.219	1655.854	1.66E-06	1.19E-07	1.46E-02
HFIR Stock 3 - Np	3.034	1082.127	1.08E-06	7.79E-08	9.52E-03
HFIR Stock 1 - U	1.232	17.072	1.71E-08	1.23E-09	1.50E-04
HFIR Stock 2 - U	1.215	16.388	1.64E-08	1.18E-09	1.44E-04
HFIR Stock 3 - U	1.028	10.665	1.07E-08	7.68E-10	9.38E-05
MURR Stock 1 - Np	2.167	147.015	1.47E-07	3.53E-09	1.14E-03
MURR Stock 2 - Np	2.158	143.968	1.44E-07	3.46E-09	1.12E-03
MURR Stock 3 - Np	2.165	146.300	1.46E-07	3.51E-09	1.13E-03
MURR Stock 1 - U	0.162	1.454	1.45E-09	3.49E-11	1.13E-05
MURR Stock 2 - U	0.162	1.452	1.45E-09	3.49E-11	1.13E-05
MURR Stock 3 - U	0.147	1.403	1.40E-09	3.37E-11	1.09E-05

Table 25. The concentration of ^{240}Pu calculated using the best-fit line for the ^{238}U standard.

^{240}Pu					
Sample Name	X (ppb in log scale)	x (ppb)	x (g/mL)	x (g)	fraction
HFIR Stock 1 - Np	2.163	145.575	1.46E-07	1.05E-08	1.28E-03
HFIR Stock 2 - Np	2.146	139.876	1.40E-07	1.01E-08	1.23E-03
HFIR Stock 3 - Np	1.967	92.582	9.26E-08	6.67E-09	8.14E-04
HFIR Stock 1 - U	0.143	1.389	1.39E-09	1.00E-10	1.22E-05
HFIR Stock 2 - U	0.116	1.305	1.31E-09	9.40E-11	1.15E-05
HFIR Stock 3 - U	-0.074	0.844	8.44E-10	6.08E-11	7.42E-06
MURR Stock 1 - Np	0.794	6.216	6.22E-09	1.49E-10	4.82E-05
MURR Stock 2 - Np	0.788	6.132	6.13E-09	1.47E-10	4.75E-05
MURR Stock 3 - Np	0.786	6.111	6.11E-09	1.47E-10	4.74E-05
MURR Stock 1 - U	-1.214	0.061	6.10E-11	1.46E-12	4.73E-07
MURR Stock 2 - U	-1.222	0.060	6.00E-11	1.44E-12	4.65E-07
MURR Stock 3 - U	-1.236	0.058	5.80E-11	1.39E-12	4.50E-07

Using the calculated information in Tables 21-25, the percentages of ^{235}U, ^{237}Np, and total Pu were determined. These results can be found in Table 26. The initial enrichment of the uranium pellet for HFIR was 0.3%, otherwise known as depleted uranium. The calculated enrichment, based on ICP-MS results, was approximately 0.3% of ^{235}U. The calculated percentage of ^{237}Np produced in HFIR was 0.004%. This is not the assumed value of 0.01% but it is expected since only ^{237}Np was considered. ^{239}Np or other isotopes were not considered in this analysis. The percentage of total Pu produced agreed with previously measured data at approximately 1.5%. The initial enrichment of the uranium pellet for MURR was natural uranium, 0.711%. The calculated enrichment, based on ICP-MS results, was approximately 0.6% of ^{235}U. The calculated percentage of ^{237}Np produced in HFIR was less than 0.001%. Again, this is not the assumed value of 0.01% but it is expected since not all isotopes of Np were considered and the MURR irradiation was expected to produce less ^{237}Np than the HFIR. The percentage of

total Pu produced agreed with previously measured data at approximately 0.1 %, which agrees with literature as well. The assumed error on these results is 10%.

Table 26. The calculated percentages of ^{235}U, ^{237}Np, and total Pu for the HFIR and MURR pellets per ICP-MS results. The assumed errors is to be less than 10%.

Sample Name	% of ^{235}U	% of ^{237}Np	% Pu to ^{238}U
HFIR Stock 1 - Np	0.285	0.004	1.615
HFIR Stock 2 - Np	0.288	0.004	1.606
HFIR Stock 3 - Np	0.285	0.004	1.582
HFIR Stock 1 - U	0.292	0.004	1.672
HFIR Stock 2 - U	0.292	0.004	1.660
HFIR Stock 3 - U	0.291	0.004	1.676
MURR Stock 1 - Np	0.591	0.00014	0.138
MURR Stock 2 - Np	0.587	0.00015	0.139
MURR Stock 3 - Np	0.593	0.00015	0.141
MURR Stock 1 - U	0.641	0.00014	0.147
MURR Stock 2 - U	0.647	0.00020	0.140
MURR Stock 3 - U	0.625	0.00018	0.137

4. A FORENSIC INVESTIGATION OF A NEPTUNIUM SPHERE USED FOR NEPTUNIUM SUBCRITCAL OBSERVATIONS AT LOS ALAMOS NATIONAL LABORATORY

During the summer of 2019 and summer of 2020, work was conducted at Los Alamos National Laboratory (LANL) to quantify impurities found in a previously cast neptunium sphere. Analysis was first conducted looking at only neutron emissions behavior and secondly, photon behavior. The neptunium sphere was approximately 6070.4 g with a diameter of 8.29 cm. [13] The purpose of this work was to aid in the analysis of previous measurements involving neptunium to better understand its neutronic behavior and to begin quantifying the impurities within the sphere.

4.1 Literature Review for $\bar{\upsilon}$ for ^{237}Np

This behavior is not well documented, as the critical mass varies with different libraries and different published values for its average number of neutrons per fission, $\bar{\upsilon}$, leading to the conclusion that more benchmarks are needed to help characterize this behavior. A literature review was conducted to determine $\bar{\upsilon}$ values for ^{237}Np – the result of this literature survey was twenty-six sources with differing values and methodologies of obtaining the values. The list of sources and the associated $\bar{\upsilon}$ value with associated error can be seen in APPENDIX C. Figure 12 and Figure 13 below show plotted $\bar{\upsilon}$ values for sources outlined in APPENDIX C. Due to the variety of values at different energies, Figure 12 plots the two values which appeared the most often; these values were $\bar{\upsilon}$ values for 1.0E-11 MeV and 1.0 MeV neutron-induced fission. Figure 13 plots the change in $\bar{\upsilon}$ values as it varies with energy in units of MeV. ENDF/B-VIII.0 has the same prompt $\bar{\upsilon}$ as a function of energy as ENDF/B-VI.1 and ENDF/B-VI.8. All three of

these libraries have only six-energy-group values which can be found in Table 27. Errors were not plotted in Figure 13 for ENDF values because the covariances are listed for a 32-energy-group and were not updated to have the same energy structure for the six-energy-group values listed in Table 27. A energy-group can be defined as the structure in which energy dependent cross-sections are grouped. Other values for $\bar{\upsilon}$ found in literature can be found in APPENDIX C.

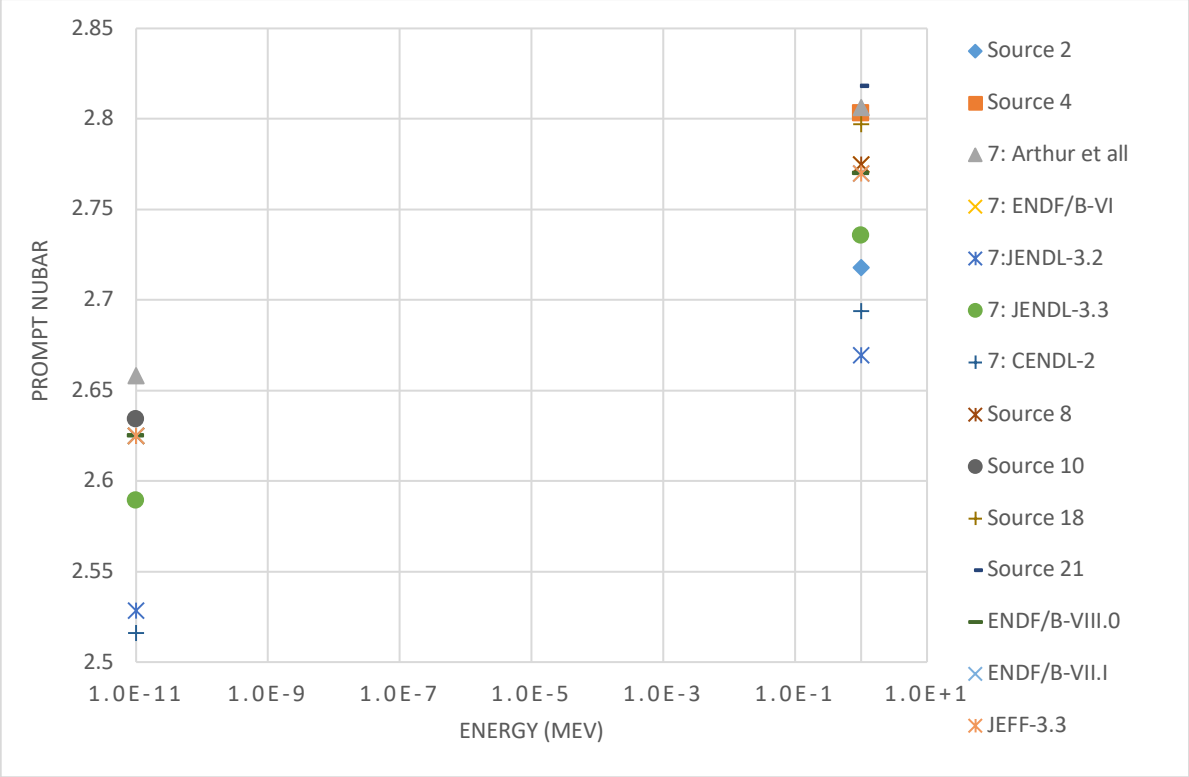

Figure 12. Prompt $\bar{\upsilon}$ values for ^{237}Np found in literature reviewed sources. No error bars are plotted because the difference in methodologies for obtaining these values.

Table 27. ENDF/B.VIII.0 Distribution for six-energy-group values for $\bar{\upsilon}$. [34] Per the IAEA nuclear data site and the KAERI nuclear data site covariances for $\bar{\upsilon}$ could not be obtained for ^{237}Np; the data was not found.

Energy [MeV]	$\bar{\upsilon}$
1.00E-11	2.625
4.00E+00	3.224
7.00E+00	3.677
1.10E+01	4.324
1.20E+01	4.466
2.00E+01	5.520

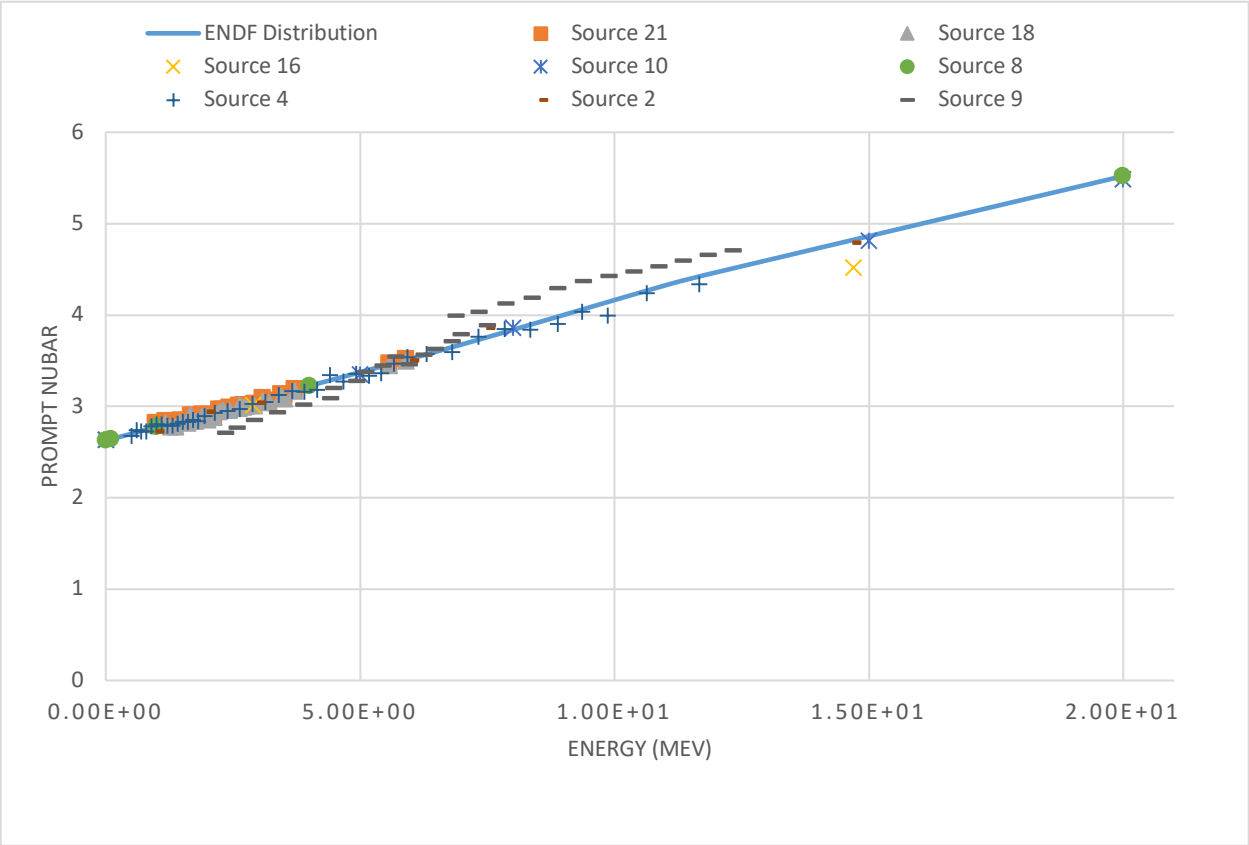

Figure 13. ENDF8 $\bar{\upsilon}$ values for ^{237}Np found in literature reviewed sources. Error bars were not plotted for ENDF8 because covariances were added in 32-energy groups but did not get updated in the underlying $\bar{\upsilon}$ data to have the same energy structure of what is plotted. [34, 35]

4.2 The Neptunium Subcritical Observation (NeSO) Benchmark Measurement Neutron Analysis

The Neptunium Subcritical Observation (NeSO) Benchmark Measurement Analysis was conducted in March 2019 by the Advanced Technologies Group, NEN-2, at the Device Assembly Facility (DAF). [36, 37] The experimental setup used to monitor this occurrence can be seen in Figure 14. The bare neptunium sphere was mounted between two LANL Neutron Multiplicity ^{3}He Array Detectors (NoMADs). It should be noted that, although the sphere is described as 'bare,' it is actually encapsulated by concentric layers of 0.261 cm of tungsten and 0.191 cm of nickel used to secure the neptunium inside. [13] This was done to reduce the gamma-radiation exposure when handling the sphere produced by ^{233}Pa, the first daughter

nuclide from ^{237}Np. [13] Each of the NoMAD arrays housed fifteen ^{3}He detectors encased in a moderation layer of polyethylene, resulting in thirty detectors in total throughout the experiment. [38]

During this benchmark, it was observed that the neutron distribution of the sphere was not uniform, which lead to the conclusion that the neptunium sphere was not 100% ^{237}Np and that there was a 'hot spot' caused from impurities located in a single spot. This hot spot caused the neutron emission rate to be higher than expected and lead to discrepancies between the simulated and experimental neutron emission rates. To verify the claim of a 'hot spot' within the sphere, the suspected location was marked with an "X" on top of the outer casing. The sphere was subsequently rotated to different angles and counted using the NoMADs. Results showed that when the "X" faced one NoMAD, the recorded neutron emission rate was higher than the rate registered by the NoMAD on the opposite side. This series of rotations showed that the 'hot spot' was at one single point on the sphere.

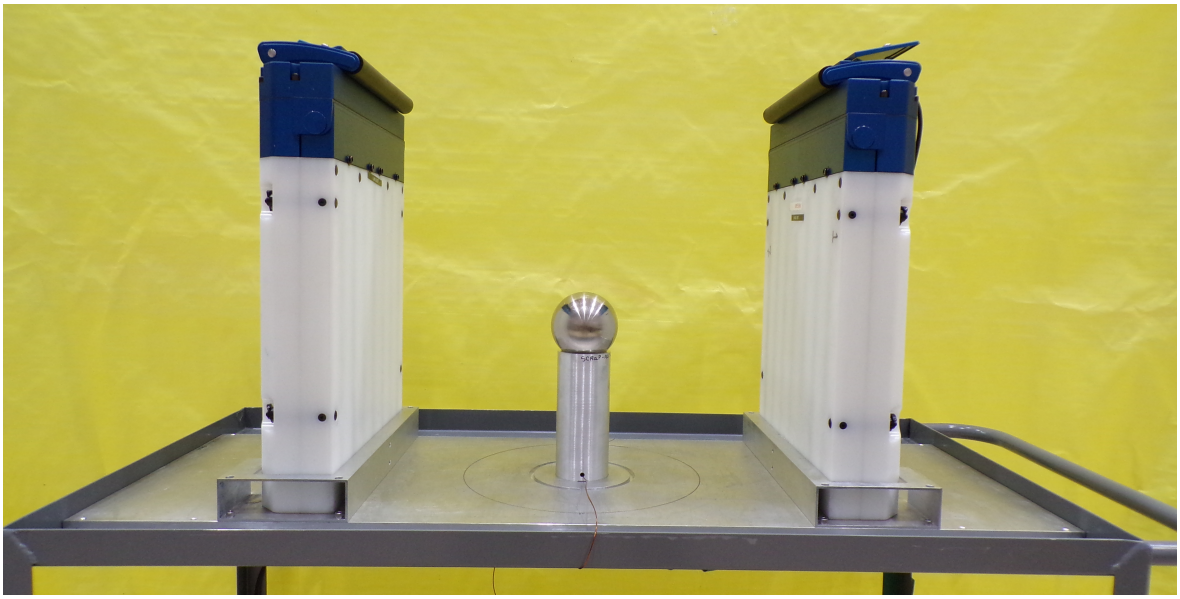

Figure 14. NeSO Experiment conducted in March of 2019, LA-UR-19-28888. The supported neptunium sphere is centered relative to the two NoMAD detectors on the left and right.

Initially the experimental set up shown in Figure 14 was modeled in *MCNP®6/6.2* using the nuclide distribution given in Table 1, which was presented in section 1.1. For simplicity, Table 1 is presented below again.

Table 1. Isotopic distribution of the neptunium sphere measured using chemical analysis on the sprue at LANL. Approximately 1% of the mass of the total sphere contents are not accounted for due to the sprue sample not dissolving to completeness. Data taken from [13].

Element	Fraction (wt. %)	Nuclide	Abundance (wt. %)
Np	98.8	^{237}Np	100
Total U	0.035	^{233}U	9.92
		^{234}U	1.61
		^{235}U	79.2
		^{236}U	0.44
		^{238}U	8.74
Total Pu	0.0355	^{238}Pu	4.45
		^{239}Pu	88.18
		^{240}Pu	6.32
		^{241}Pu	0.17
		^{242}Pu	0.89
Am	Trace	^{241}Am	6.0 ppm
		^{243}Am	1823.0 ppm

However, the *MCNP®6/6.2* model had to be revised due to the found 'hot spot,' which was suspected to be caused by impurities in the sphere. Through gamma spectrometry, the impurities in the Np sphere were observed to contain ^{244}Cm, ^{239}Np, and ^{243}Am. These nuclides were not previously identified during the initial chemical analysis of the Np sphere contents, therefore, they were not taken into account during the modeling of the Np sphere. This could be caused by the sprue not fully dissolving to completeness during analysis.

Due to the uncertainty in the quantity of each nuclide present in the hot spot, a Python script was written to generate inputs that incrementally changed the amount of ^{244}Cm in the system. It was determined that the ^{239}Np and ^{243}Am had no contribution to the neutron multiplicity counts due to no statistically measurable effects in the simulation results. The ^{243}Am

alpha decays into ^{239}Np and has gamma signatures, but no significant effects on the overall neutron emission rate. The Python script added the impurities to a spot modeled in the simulation, shown in Figure 15, that was made by 'cutting' a hole 2 mm deep and creating a spot with a mass of 5.25 g, assuming that the remainder of the sphere was 5,994.75 g of pure ^{237}Np. The ^{244}Cm impurity fraction that resulted in the most reasonably close emission rate to the experimental data was somewhere between 0.034-0.035% assuming the mass given above.

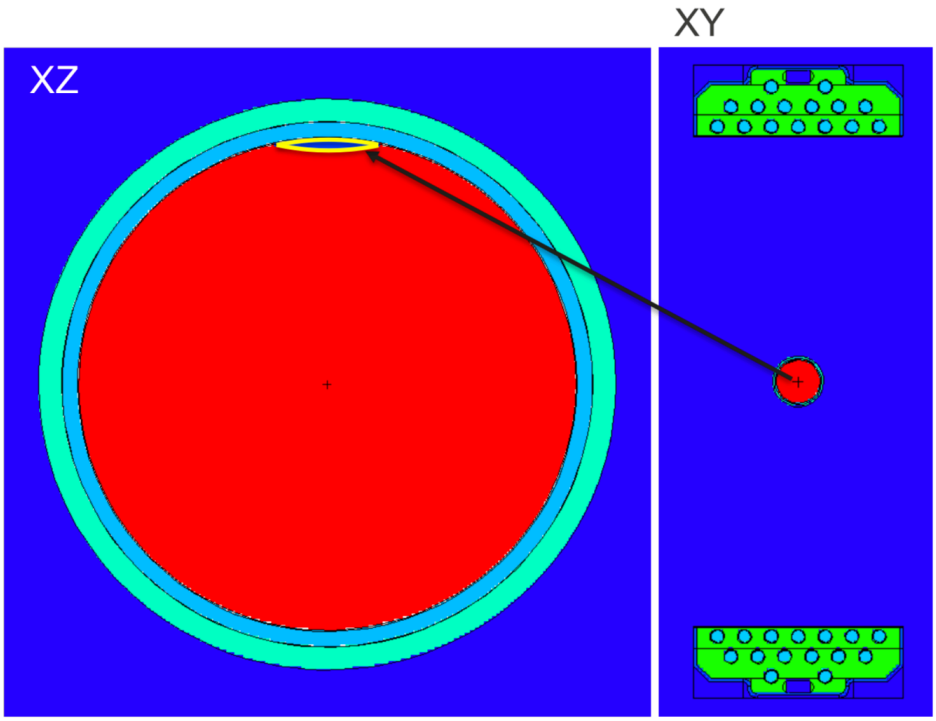

Figure 15. A visual representation of the modeled hot spot accomplished by 'cutting' a hole 2 mm deep and creating a spot with a mass of 5.25 g. Made using VisEd in Summer of 2019, LA-UR-19-27546.

4.3 The Neptunium Subcritical Observation (NeSO) Benchmark Measurement Photon Analysis

During the summer of 2019, neutron analysis was preformed using model and simulation manipulation to estimate how much ^{244}Cm could be present in the neptunium sphere used in the Neptunium Subcritical Observation (NeSO) Benchmark at LANL. There was interest in observing if the photon data confirmed a similar impurity amount or if it disputed the original neutron impurity. During a summer internship in 2020, efforts were performed to model the photon emission during the observational experiment.

Gamma measurements were performed in three different ways during the experiment: 1) the bare Np sphere was measured for two hours using a gamma detector known as Detective X at the same height as the sphere, four meters from the detector face; 2) the bare Np sphere with the hot spot pointing towards the detector face was counted for 7,200 s where the detector was at the same height, four meters away; and 3) the bare Np sphere with the hot spot pointing away from the detector face with the same parameters as the previous measurement. Note that although the sphere is described as 'bare,' it is encapsulated by concentric layers of 0.261 cm of tungsten and 0.191 cm of nickel. [13] These layers will affect the gamma measurements since the tungsten and nickel reduce the gamma-radiation exposure when handling the sphere. [13]

To simplify modeling and simulation efforts a combination of *MCNP®6/6.2* and The Gamma Detector Response and Analysis Software tool (GADRAS) was utilized to simulate the HPGe gamma spectrum for the detective X detector. The purpose of this was to utilize the *MCNP®6/6.2* neutron and photon transport simulations coupled with the GADRAS detector response calculations to produce realistic estimations of the full gamma spectrum [39] given by the bare Np sphere and gamma spectra scenarios outlined above. However, the *MCNP®6/6.2*

output needed to be converted to a .gam file for compatibility with GADRAS. This process can be found in Appendix D.

5. SUMMARY AND CONCLUSIONS

Neptunium is believed to be weapons-useable and is not currently supervised under IAEA safeguard protocols; however, Np needs to be considered as separation of this nuclide and reactor waste production continue to increase. A literature review showed that the critical mass of ^{237}Np varied among different libraries and published values for its average number of neutrons per fission, $\bar{\upsilon}$. Los Alamos National Laboratory previously concluded that the estimated critical mass of ^{237}Np was approximately 60 kg, but more research and benchmarks are needed to make definite conclusions regarding the neutronic behavior of ^{237}Np.

Neptunium-237 has a fast neutron fission cross section comparable to that of ^{239}Pu, and its production mass fraction is roughly 0.1% of used nuclear fuel. Although the amount of ^{237}Np produced is low, the growing trove of used nuclear fuel is a proliferation risk, especially if the separation of long-lived actinides becomes an industry standard. Production of ^{237}Np was evaluated using *ORIGEN2.0* to simulate one ton of various fuels for varying reactor types. Burnup simulations comparisons were also made between data points to monitor the overall production for a given reactor. Based on the results, it was determined that PWRs produced the most ^{237}Np, followed by BWRs, CANDU reactors, and FBRs.

Pressurized water reactors and BWRs have a higher ^{235}U content than a CANDU, which burn natural uranium, and FBRs, which burn depleted uranium, thus, further supporting these results. Comparisons were also made with unique uranium samples irradiated at the HFIR and at the MURR. These samples were irradiated at low burnup conditions and experimentally designed to mimic the irradiation of a FBR and CANDU. Analyses of these was performed and analyzed using ICP-MS to quantify how much ^{237}Np was produced in these irradiated samples.

For comparison, the PWR, BWR, FBR, and CANDU reactors were modeled for low burnup conditions of 5,000 MWd/MTU to compare the production rates.

ICP-MS results demonstrated that an average of 0.004% of ^{237}Np was present in the HFIR sample (burnup less than 4,500 MWd/MTU) and an average of less than 0.001% of ^{237}Np was present in the MURR sample (burnup about 1,000 MWd/MTU). Although the amount of neptunium produced was in low concentrations, this result and study is useful when analyzing low burnup waste streams and further show that in large troves the amount of ^{237}Np present is of a proliferation risk or concern. Given these results, it is recommended that the IAEA needs to develop further safeguards measures to monitor the production and quantity of ^{237}Np present in fuel and fuel waste streams to ensure material accountancy and control of all special nuclear material, especially those of a weapons concern.

A literature review was conducted to determine $\bar{\upsilon}$ values for ^{237}Np – the result of this literature survey was twenty-six sources with differing values and methodologies of obtaining the values. The neptunium sphere was approximately 6070.4 g with a diameter of 8.29 cm. Through gamma spectrometry, the impurities in the Np sphere were observed to contain ^{244}Cm, ^{239}Np, and ^{243}Am. The Python script added the impurities to a spot modeled in the simulation, shown in Figure 15, that was made by 'cutting' a hole 2 mm deep and creating a spot with a mass of 5.25 g, assuming that the remainder of the sphere was 5994.75 g of pure ^{237}Np. The ^{244}Cm impurity fraction that resulted in the most reasonably close emission rate to the experimental data was somewhere between 0.034-0.035% assuming the mass given above.

REFERENCES

[1] G. R. Eppich, Bulletin of the Atomic Scientists **76**, 263 (2020). doi:10.1080/00963402.2020.1806587

[2] B. Mahanty, A. Bhattacharyya, and P. K. Mohapatra, Journal of Chromatography A **1564**, 94 (2018). doi:10.1016/j.chroma.2018.06.026

[3] B. Goddard, A. Solodov, and V. Fedchenko, The Nonproliferation Review **23**, 677 (2017). doi:10.1080/10736700.2017.1339934

[4] M. L. Garcia, *The Design and Evaluation of Physical Protection Systems*, Second Edition ed., (Amorette Pedersen, Butterworth-Heinemann, 2008).

[5] S. J. Goldstein, K. A. Hinrichs, A. J. Nunn, D. W. Gurganus, R. S. Amato, and W. J. Oldham, Journal of Radioanalytical and Nuclear Chemistry **318**, 695 (2018). doi:10.1007/s10967-018-6045-4

[6] B. Goddard, in *Nuclear Engineering Department* (Texas A&M University, 2013).

[7] C. A. Wells, W. D. Stanbro, and W. S. Charlton, *Monitors for Prediction of Neptunium and Americium Concentrations in Spent Fuel*, presentation to 23rd ESARDA Symposium on Safeguards and Nuclear Material Management, Bruges, Belgiuum,

[8] Y. Shi, X. Yi, H. Zhang, T. Bai, X. He, J. Zhang, and J. Xu, Journal of Radioanalytical and Nuclear Chemistry **307**, 1215 (2015). doi:10.1007/s10967-015-4238-7

[9] V. I. Marchenko, V. S. Koltunov, O. A. Savilova, and G. I. Zhuravleva, Radiochemistry **43**, 276 (2001).

[10] F. L. Moore, Analytical Chemistry **29**, 941 (1957). doi:10.1021/ac60126a023

[11] IAEA, International Nuclear Verification Series No. 3, 2001).

[12] T. Burr, W. D. Stanbro, and W. Charlton, Journal of Nuclear Science and Technology **38**, 209 (2012). doi:10.1080/18811248.2001.9715023

[13] R. Sanchez, D. Loaiza, R. Kimpland, D. Hayes, C. Cappiello, and M. Chadwick, Nuclear Science and Engineering **158**, 1 (2017). doi:10.13182/nse08-a2734

[14] P. Weiss, Science News **162** (2002).

[15] E. R. Bertelsen, J. A. Jackson, and J. C. Shafer, Solvent Extraction and Ion Exchange, 1 (2020). doi:10.1080/07366299.2020.1720958

[16] A. Morgenstern, C. Apostolidis, R. Carlos-Marquez, K. Mayer, and R. Molinet, Radiochimica Acta **90** (2002). doi:10.1524/ract.2002.90.2_2002.81

[17] L. Perna, F. Bocci, L. Aldave de las Heras, J. De Pablo, and M. Betti, J. Anal. At. Spectrom. **17**, 1166 (2002). doi:10.1039/b202451a

[18] G. Uchiyama, T. Asakura, S. Hotoku, and S. Fujine, Solvent Extraction and Ion Exchange **16**, 1191 (1998). doi:10.1080/07360299808934576

[19] J. H. Saling and A. W. Fentiman, *Radioactive Waste Management*, Second ed., (Taylor & Francis, 2001), p^pp. 110-111, 114-117.

[20] M. Benedict, T. H. Pigford, and H. W. Levi, *Nuclear Chemical Engineering* Second ed.

[21] M. F. Vitha, *Chromatography: Principles and Instrumentation*, p^pp. 1-50.

[22] S. S. Chirayath, J. M. Osborn, and T. M. Coles, Science & Global Security **23**, 48 (2015). doi:10.1080/08929882.2015.996079

[23] K. J. Glennon, J. M. Osborn, J. D. Burns, E. D. Kitcher, S. S. Chirayath, and C. M. Folden III, Journal of Radioanalytical and Nuclear Chemistry **320**, 405 (2019). doi:10.1007/s10967-019-06486-w

[24] E. D. Kitcher, J. M. Osborn, and S. S. Chirayath, Nuclear Engineering and Technology **51**, 1355 (2019). doi:10.1016/j.net.2019.02.019
[25] J. M. Osborn, K. J. Glennon, E. D. Kitcher, J. D. Burns, C. M. Folden III, and S. S. Chirayath, Nuclear Engineering and Technology **50**, 820 (2018). doi:10.1016/j.net.2018.04.017
[26] J. M. Osborn, K. J. Glennon, E. D. Kitcher, J. D. Burns, C. M. Folden III, and S. S. Chirayath, Nuclear Engineering and Technology **51**, 384 (2019). doi:10.1016/j.net.2018.11.003
[27] J. M. Osborn, E. D. Kitcher, J. D. Burns, C. M. Folden III, and S. S. Chirayath, Nuclear Technology **201**, 1 (2017). doi:10.1080/00295450.2017.1401442
[28] M. W. Swinney, C. M. Folden III, R. J. Ellis, and S. S. Chirayath, Nuclear Technology **197**, 1 (2017). doi:10.13182/nt16-76
[29] e. a. C.J. Werner, Computer Code MCNP6.2 RELEASE NOTES.
[30] C. J. Werner(editor), Computer Code MCNP USERS MANUAL - CODE VERSION 6.2.
[31] J. P. Faris and R. F. Buchanan, Analytical Chemistry **36**, 1157 (1964).
[32] S. F. Marsh, J. E. Alarid, C. F. Hammond, M. J. McLeod, F. R. Roensch, and J. E. Rein, 9 (1978).
[33] J. M. Osborn, K. J. Glennon, E. D. Kitcher, J. D. Burns, C. M. Folden III, and S. S. Chirayath, Nuclear Engineering and Technology **51**, 384 (2019). doi:https://hdl.handle.net/10.1016/j.net.2018.11.003
[34] M. B. C. D.A.Brown, R.Capote, A.C.Kahler, A.Trkov, M.W.Herman, A.A.Sonzogni, Y.Danon, A.D.Carlson, M.Dunn, D.L.Smith, G.M.Hale, G.Arbanas, R.Arcilla, C.R.Bates, B.Beck, B.Becker, F.Brown, R.J.Casperson, J.Conlin, D.E.Cullen, M.-A.Descalle, R.Firestone, T.Gaines, K.H.Guber, A.I.Hawari, J.Holmes, T.D.Johnson, T.Kawano, B.C.Kiedrowski, A.J.Koning, S.Kopecky, L.Leal, J.P.Lestone, C.Lubitz, J.I.Márquez Damián, C.M.Mattoon, E.A.McCutchan, S.Mughabghab, P.Navratil, D.Neudecker, G.P.A.Nobre, G.Noguere, M.Paris, M.T.Pigni, A.J.Plompen, B.Pritychenko, V.G.Pronyaev, D.Roubtsov, D.Rochman, P.Romano, P.Schillebeeckx, S.Simakov, M.Sin, I.Sirakov, B.Sleaford, V.Sobes, E.S.Soukhovitskii, I.Stetcu, P.Talou, I.Thompson, S.Van Der Marck, L.Welser-Sherrill, D.Wiarda, M.White, J.L.Wormald, R.Q.Wright, M.Zerkle, G.Žerovnik, Y.Zhu, Computer Code ENDF/B-VIII.0: THE 8TH MAJOR RELEASE OF THE NUCLEAR REACTION DATA LIBRARY WITH CIELO-PROJECT CROSS SECTIONS, NEW STANDARDS AND THERMAL SCATTERING DATA.
[35] M. H. M.B. Chadwick, P. Obložinský, M.E. Dunn, Y. Danon, A.C. Kahler, D.L. Smith, B. Pritychenko, G. Arbanas, R. Arcilla, R. Brewer, D.A. Brown, R. Capote, A.D. Carlson, Y.S. Cho, H. Derrien, K. Guber, G.M. Hale, S. Hoblit, S. Holloway, T.D. Johnson, T. Kawano, B.C. Kiedrowski, H. Kim, S. Kunieda, N.M. Larson, L. Leal, J.P. Lestone, R.C. Little, E.A. McCutchan, R.E. MacFarlane, M. MacInnes, C.M. Mattoon, R.D. McKnight, S.F. Mughabghab, G.P.A. Nobre, G. Palmiotti, A. Palumbo, M.T. Pigni, V.G. Pronyaev, R.O. Sayer, A.A. Sonzogni, N.C. Summers, P. Talou, I.J. Thompson, A. Trkov, R.L. Vogt, S.C. van der Marck, A. Wallner, M.C. White, D. Wiarda, P.G. Young, Computer Code ENDF/B-VII.1: NUCLEAR DATA FOR SCIENCE AND TECHNOLOGY: CROSS SECTIONS, COVARIANCES, FISSION PRODUCT YIELDS AND DECAY DATA.
[36] A. McSpaden, T. E. Cutler, R. Bahran, and J. D. Hutchinson, Transactions of the American Nuclear Society **119**, 781 (2018).

[37] R. Bahran, T. Cutler, and J. Hutchinson, Transactions of the American Nuclear Society **117**, 853 (2017).
[38] J. Arthur, R. Bahran, J. Hutchinson, A. Sood, N. Thompson, and S. A. Pozzi, Progress in Nuclear Energy **106**, 120 (2018).
[39] M. W. Rawool-Sullivan, J. K. Mattingly, D. J. Mitchell, and J. D. Hutchinson, edited by C. M. G. S. o. H. G. Spectrum.
[40] M. Rawool-Sullivan, *Generating a gam file using MCNP5, LA-UR-11-00039*, presentation to

APPENDIX A

ORIGEN2.0 INPUT FILE FOR A PWR USING US LIBRARIES FOR HIGH BURNUP

The ORIGEN2.0 input below indicates which libraries are being used the fuel composition and the number of days it takes to achieve a given burnup. In this example it took 1200.0 days to achieve the intended discharge burnup of 45,000 MWd/MTU.

```
-1
-1
-1
  RDA  Irradiation of 1 MT of PWR fuel
  RDA  Fuel enrichment is 3.0 w/o U-235
  RDA  Irradiation using libraries for PWRUS
  RDA  Overwrites Vector 2
  RDA
  LIB  0  1 2 3  601 602 603  9  50 0 1 38
  PHO     101 102 103  10
  INP  1   1  -1  -1   1   1
  BUP
  IRP 100.0 37.5 1 2 4 2 BURNUP=3,750 MWD/MT
  IRP 200.0 37.5 2 2 4 0 BURNUP=7,500 MWD/MT
  IRP 300.0 37.5 2 2 4 0 BURNUP=11,250 MWD/MT
  IRP 400.0 37.5 2 2 4 0 BURNUP=15,000 MWD/MT
  IRP 500.0 37.5 2 2 4 0 BURNUP=18,750 MWD/MT
  IRP 600.0 37.5 2 2 4 0 BURNUP=22,500 MWD/MT
  IRP 700.0 37.5 2 2 4 0 BURNUP=26,250 MWD/MT
  IRP 800.0 37.5 2 2 4 0 BURNUP=30,000 MWD/MT
  IRP 900.0 37.5 2 2 4 0 BURNUP=33,750 MWD/MT
  IRP 1000.0 37.5 2 2 4 0 BURNUP=37,500 MWD/MT
  IRP 1100.0 37.5 2 2 4 0 BURNUP=41,250 MWD/MT
  IRP 1200.0 37.5 2 2 4 0 BURNUP=45,000 MWD/MT
  DEC 1300.0      2 3 4 0 DECAY FOR 100.0 DAYS
  DEC 2395.0      3 4 4 0 DECAY FOR 3 YEARS
  DEC 3125.0      4 5 4 0 DECAY FOR 5 YEARS
  DEC 4950.0      5 6 4 0 DECAY FOR 10 YEARS
  BUP
  OPTL 8 8 8 8 8 8 8 8 8 8 7*8 5*8 8
  OPTA 8 8 8 8 2 8 7 8 7 8 8 7*8 5*8 8
  OPTF 8 8 8 8 7 8 7 8 7 8 8 7*8 5*8 8
  OUT     6   1  -1   0
  END
2 922340 270. 922350 30000. 922380 969730. 80160 1186.
0
```

APPENDIX B

ORIGEN2.0 INPUT FILE FOR A PWR USING US LIBRARIES FOR LOW BURNUP

The ORIGEN2.0 input below indicates which libraries are being used (line indicated by 'LIB'), the fuel composition and the number of days it takes to achieve

```
-1
-1
-1
  RDA  IRRADIATION OF 1 MT OF PWR FUEL
  RDA  FUEL ENRICHMENT IS 3.0 W/O U-235
  RDA  IRRADIATION FOR PWRUS LIBRARIES
  RDA  BURNUP=5,000 MWD/MT, DECAY FOR 7 YRS
  RDA
  LIB  0  1 2 3  601 602 603  9  50 0 1 38
  PHO    101 102 103  10
  INP  1  1  -1  -1  1  1
  BUP
  IRP  26.67 37.5 1 2 4 2 BURNUP=1,000 MWD/MT
  IRP  53.33 37.5 2 2 4 0 BURNUP=2,000 MWD/MT
  IRP  80.00 37.5 2 2 4 0 BURNUP=3,000 MWD/MT
  IRP 106.67 37.5 2 2 4 0 BURNUP=4,000 MWD/MT
  IRP 133.33 37.5 2 2 4 0 BURNUP=5,000 MWD/MT
  DEC 2688.33     2 3 4 0 DECAY FOR 7 YEARS
  BUP
  OPTL 8 8 8 8 8 8 8 8 8 8 7*8 5*8 8
  OPTA 8 8 8 8 2 8 7 8 7 8 8 7*8 5*8 8
  OPTF 8 8 8 8 7 8 7 8 7 8 8 7*8 5*8 8
  OUT    3   1   -1   0
  END
2 922340 270. 922350 30000. 922380 969730. 80160 1186.
0
```

APPENDIX C

NEPTUNIUM $\bar{\upsilon}$ LITERATURE REVIEW

Last Updated: June 25, 2019

Legend:

Summary Table:
*= Interpolated Value
*= AVG - Average Value over a given energy range
ORANGE = For Delayed Neutron Measurements
PURPLE = Prompt Neutron Measurements

References:
BLUE = Found and Listed
RED = Search For
GREEN = Evaluations were based on calculations and/ or measurements seen in papers (comparison of data listed in publication)

Summary Values for Nubar					
#	Title	Energy (MeV)	Nubar		Δ Nubar
1	Measurements Results of Average Neutron Multiplicity from Neutron Induced Fission of Actinides in 0.5-10 MeV Energy Range				
2	Prompt neutrons from neutron-induced fission of ^{237}Np	1.0	2.718		0.057
3	Neutrons and Radiations from Fission *Proceedings of the Second United Nations International Conference on the Peaceful Uses of Atomic Energy*	AVG	Topsy*	2.81	0.09
			Jezebel*	2.90	0.04
4	THE ENERGY DEPENDENCE MEASUREMENTS OF AVERAGE NUMBER OF PROMPT NEUTRONS FROM NEUTRON-INDUCED FISSION OF U-235, NP-237 AND PU-240 FROM 0.5 TO 12 MEV	1.0	2.803		0.027
5	Prompt-$\bar{\upsilon}$ Calculations for 53 Actinides				
6	Review and Assessment of Neutron Cross Section and $\bar{\upsilon}$ Covariances for Advanced Reactor Systems				
7	Analysis of Np-237 ENDF for the Theoretical Interpretation of Critical Assembly Experiments (Also includes $\bar{\upsilon}$ —delayed values in table)	1.0E-05 (eV)	2.6582 2.62500 2.5284 2.5894 2.5162		-
		1.0	2.80620		-

			2.77481 2.66968 2.73580 2.69389	
8	Section 12.0 Useful Tables – Nuclear Weapons Frequently Asked Questions	1.0E-05 (eV)	2.625	-
		1.0	2.775	-
		20	5.521	-
9	Mesure de ν_p et E_γ, pour la fission de ^{232}Th, ^{235}U, et ^{237}Np induite par des neutrons d'energie comprise entre 1 et 15 MeV			
10	Neutron Data Evaluation of ^{237}Np (2010)	1.0E-05 (eV)	2.6343	0.155
		20	5.4880	0.664
11	An Integrated System for Production of Neutronics and Photonics Calculational Constants Volume 15, Part B. THE LLL EVALUATED-NUCLEAR-BATA LIBRARY (ENDL): GRAPHS OFCROSS SECTIONS FROM THE LIBRARY			
12	Neutron Cross Sections, Vol. 1, Part B., Academic Press, INC. (1984).	AVG	2.525*	0.06
13	Measurements of Delayed-Neutron Yields from Thermal-Neutron-Induced Fission of 235U, 233U, 239Pu, and 237Np*			
14	Delayed Neutron Measurements from Neutron Induced Fission of ^{235}U, ^{233}U, ^{239}Pu, and ^{237}Np			
15	Mean Number of Neutrons From Fast Fission of 237Np	AVG	2.96*	0.05
16	Neutron spectra in fission of 237Np by the neutrons with energies 2.9 and 14.7 MeV			
17	The Number of Prompt Neutrons in the Fission of U-235, U-233, Th-233, and Np-237 by Fast Neutrons	AVG	2.72*	0.15
18	Discrepancy of the Results of prompt-$\bar{\nu}$ measurements in the fission of 237Np nuclei by neutrons	1.0	2.797105*	
19	Analysis of prompt fission neutron spectrum and multiplicity for ^{237}Np(n,f) in the frame of multi-modal Los Alamos model			
20	Improved Los Alamos model applied to the neutron induced fission of ^{235}U and ^{237}Np	AVG	2.1835*	

21	Measurements of the Energy Dependence of the Mean Number of Prompt Neutrons in Neutron-Induced Fission of 237Np Nuclei	1.0	2.818105*	
22	Measurements of the average energy and multiplicity of prompt-fission neutrons from 238U(n,f) and 237Np(n,f) from 1 to 200 MeV			
23	Multiplicities of Fission Neutrons*	-	-	-
24	ENDF/B-VIII.0	1.0E-05 (eV)	2.625	-
		1.0	2.77*	-
		20	5.5207	-
25	JEFF-3.3	1.0E-05 (eV)	2.625	-
		1.0	2.77*	-
		20	5.5207	-
26	ENDF/B-VII.I	1.0E-05 (eV)	2.625	-
		1.0	2.77*	-
		20	5.5207	-

FIGURE 1. Prompt $\bar{\nu}$ values for ^{237}Np found in literature reviewed sources. No error bars are plotted because the difference in methodologies for obtaining these values.

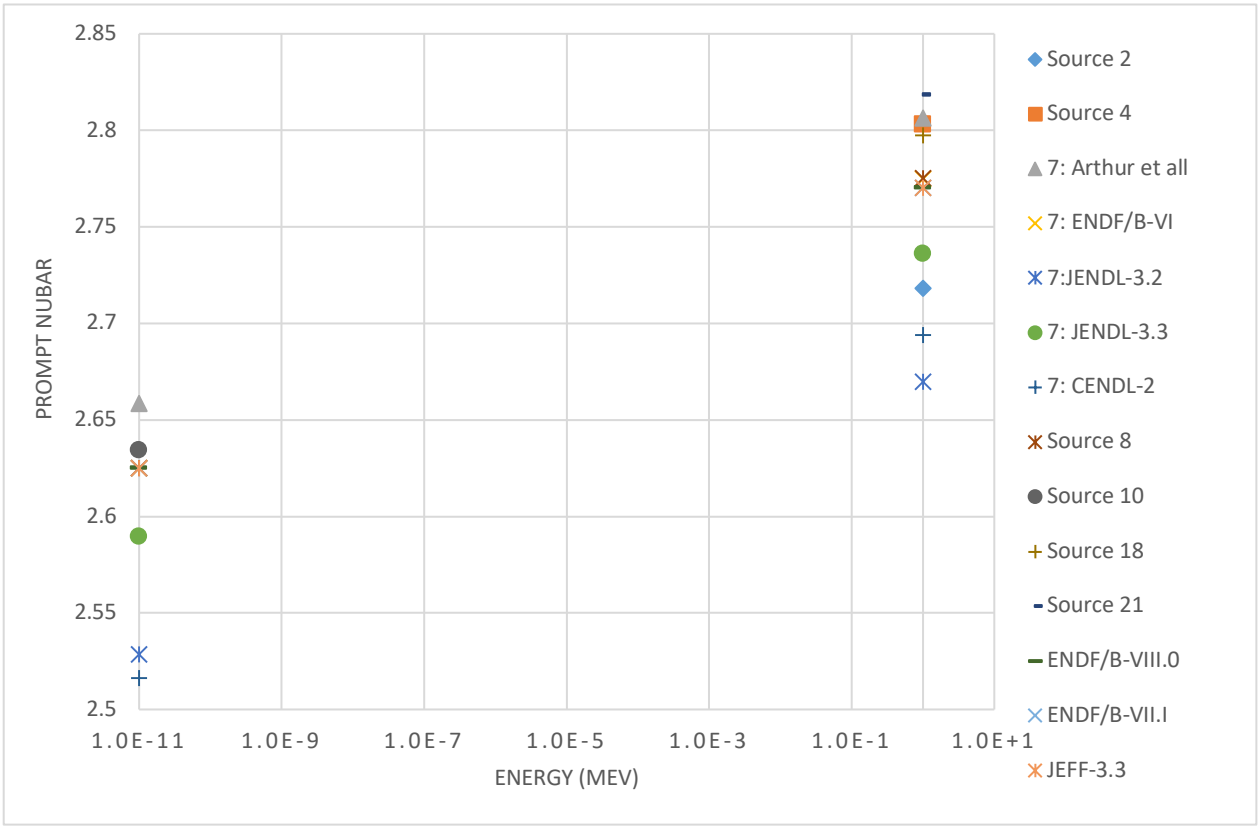

FIGURE 2. Plotted curve for ENDF8 $\bar{\upsilon}$ values for ^{237}Np found in literature reviewed sources. No error bars were plotted for ENDF8 because covariances were added in 32 energy groups but did not get updated in the underlying $\bar{\upsilon}$ data to have the same energy structure of what is plotted.

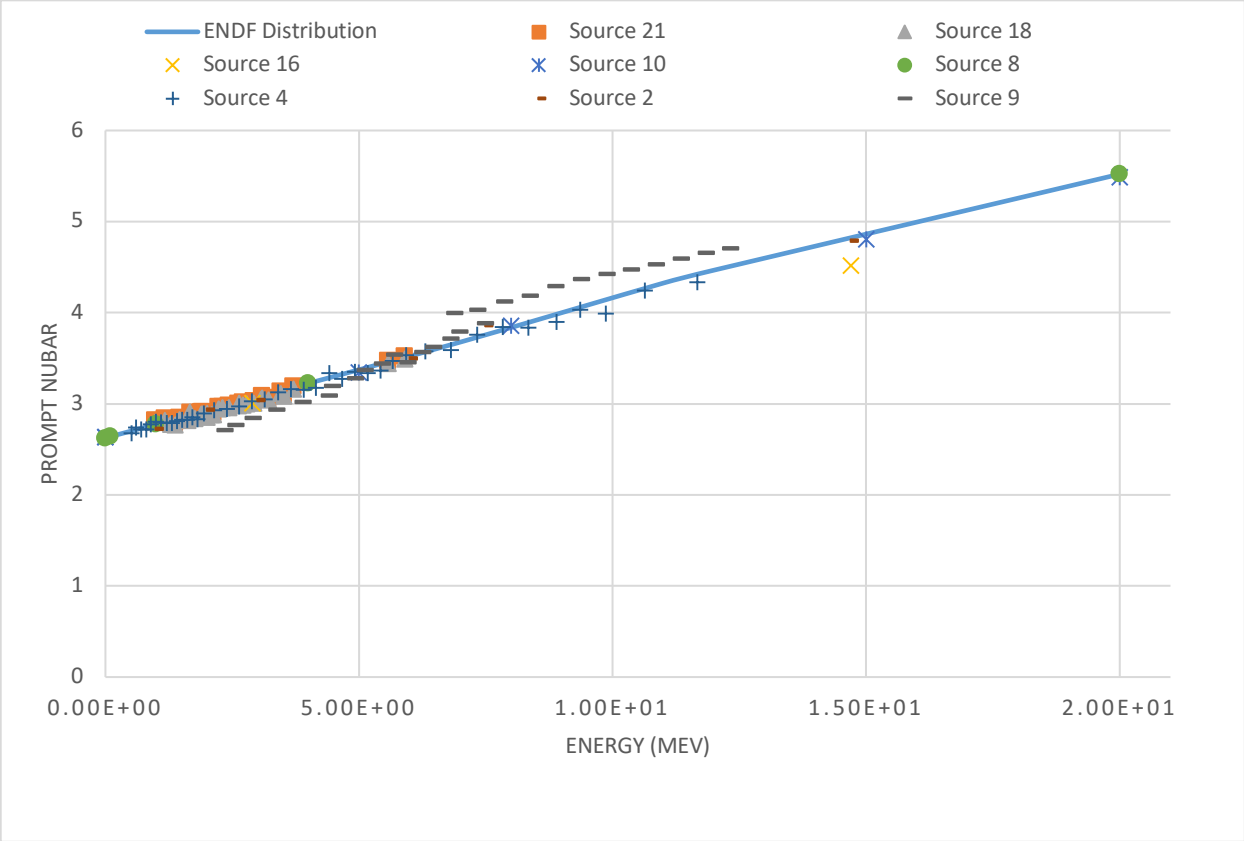

1.

Title	Measurements Results of Average Neutron Multiplicity from Neutron Induced Fission of Actinides in 0.5-10 MeV Energy Range
Author(s)	Yu.A. Khoklov, I.A. Ivanin, V.I. In'kov, Yu.I. Vinogradov, L.D. Danilin, B.N. Polunov
References Other Papers	7. J. Frehaut, A. Bertin, R. Bois, Mesure de ν_p et E_γ, pour la fission de ^{232}Th, ^{235}U, et ^{237}Np induite par des neutrons d'energie comprise entre 1 et 15 MeV., Proc. Of the Intern. Conf. on Nuclear Data for science and technology., Antwerp, Belgium, September, 1982, p.78-81., (1983). 8. L.R. Veeser, Phys. Rev. C., **17**, 385-387 (1978) 9. V.V. Malinovsky, M.Z. Tarasko, B.D. Kuzminov, V.G. Vorobyova, Atomnaya Energiya, **54**, 208, (1983).
Value	Verified Results from Sources
Figure(s)	Pg. 274, Fig. 5.
Location	TA03-207 – Library: QC770.N473 (1994)

2.

Title	Prompt neutrons from neutron-induced fission of ^{237}Np
Author(s)	L. R. Veeser
References Other Papers	10. G.F. Hansen, quoted by R.B. Leachman, in *Proceedings of the Second United Nations International Conference on the Reaceful Uses of Atomic Energy* (United Nations, Geneva, 1958), Vol. 15, P. 331. ****LOCATED In TA03-207 – Library: QC770.153 (1958)**** 11. B.D. Kuz'minov, L.S. Kutsaeva, and I.I. Bondarenko, At. Energy 4, 187 (1958) [Sov. J. At. Energy 4, 250 (1958)]. 12. V.I. Lebedev and V.I. Kalashnikova, At. Energy 10, 371 (1961) [Sov. J. At. Energy 10. 357 (1961)]. 13. R.J. Howerton, D.E. Cullen, M.H. MacGregor, s.T. Perkins, and E.F. Plechaty, Lawrence Livermore Laboratory Report No. UCRL-50400, 1976 (unpublished), Vol. 15, Part B. 14. D.I. Garber and C. Brewster, Brookhaven National Laboratory Report No. BNL 17100 (ENDF-200), 1975 (unpublished), 2nd ed.
Value	A least squares fit to the results gives $\bar{\nu}_p = 2.605 \pm 0.153E_n$ (MeV)

TABLE I. Average number of prompt neutrons per event from neutron-induced fission of ^{237}Np and the uncertainties in the measurements. A least squares fit to the results gives $\bar{\nu}_p = 2.605 + 0.153E_n$ (MeV).

E_n (MeV)	$\bar{\nu}_p$	Statistical uncertainty	Total uncertainty
1.0 ± 0.11	2.718	0.057	0.063
2.0 ± 0.08	2.934	0.057	0.064
3.0 ± 0.06	3.037	0.056	0.064
6.0 ± 0.13	3.495	0.052	0.063
7.5 ± 0.09	3.856	0.055	0.067
14.7 ± 0.15	4.785	0.071	0.085

Figures	Table 1. and FIG. 1.
Location	Phys. Rev. C., **17**, 385-387 (1978)

3.

Title	Neutrons and Radiations from Fission *Proceedings of the Second United Nations International Conference on the Peaceful Uses of Atomic Energy*
Author(s)	G.F. Hansen, quoted by R.B. Leachman
References Other Papers	6. C. block, Phys. Rev., 93, *93*, 1094 (1954). 13. R. Ra,anna and P.N. Rama Rao, *The Angular Distribution of Prompt Neutrons Emitted in the Fission of U^{235},* P/1633, the Volume, these Proceedings.
Value	**Assembly** / **$\bar{\nu}$ for ^{237}Np** Topsy / 2.81 ± 0.09 Godiva / Jezebel / 2.90 ± 0.04
Figures	Table 2. pg. 336
Location	TA03-207 – Library: QC770.153 (1958)

4.

Title	THE ENERGY DEPENDENCE MEASUREMENTS OF AVERAGE NUMBER OF PROMPT NEUTRONS FROM NEUTRON-INDUCED FISSION OF U-235, NP-237 AND PU-240 FROM 0.5 TO 12 MEV
Author(s)	Ju. A. Khokhlov, I. A. Ivanin, Ju. I. Vinogradov, V. I. In'kov, L. D. Danilin, V. I. Panin, V. N. Polynov
References Other Papers	"Existing experimental data for Np237 display systematic discrepancy [1-3]" 1. L. R. Veeser. Prompt neutrons from neutron-indused fission of Np-237// Phis. Rev. C - 1978. - v. 17., - p.385-387. 2. J. Freaut, A. Bertin, R. Bois Mesure de Yp et E , pour la fission de Th-232, U-235 et Np237 induite par des neutrons d'energie comprise entre 1 et

15 MeV.// In: Proc. of the Intern. conf. on Nuclear Data for science and tecnology., (Antwerp, Belgium, September, 1982). - 1983 - p.78-81.
3. B. r. Bopo6beBa, B. *R.* Ky3bMHHOB, B, B. MajiHHOBCKHft H flp. H3MepeHne cpepero MHcia Mr.HOBeHHHX HeHTpoHOB npH flejieHMH
Hflep Np-237 HeHTpOHaMH.// BonpOCH aTOMHOH HaVKH H TeXHHKH.Gep. flflepHbie KOHCTaHTbi, - 1980, - Bbin.3(38), c. 45-58.

Value

Np-237		
$\bar{E}$	$\bar{\nu}$	$\overline{\Delta\nu}$
0.51	2.677	0.037
0.61	2.74	0.023
0.7	2.722	0.023
0.8	2.723	0.023
0.9	2.778	0.022
1	2.803	0.027
1.1	2.8	0.019
1.21	2.787	0.023
1.31	2.787	0.022
1.41	2.811	0.027
1.51	2.828	0.027
1.61	2.828	0.024
1.71	2.854	0.027
1.81	2.835	0.022
1.94	2.895	0.018
2.14	2.929	0.025
2.39	2.948	0.023
2.64	2.974	0.027
2.89	3.026	0.022
3.14	3.047	0.021
3.4	3.127	0.035
3.66	3.165	0.034
3.91	3.157	0.05
4.15	3.18	0.039
4.41	3.34	0.031
4.67	3.272	0.039
4.92	3.353	0.05
5.17	3.338	0.046
5.42	3.365	0.048
5.67	3.47	0.05
5.93	3.538	0.049
6.31	3.576	0.049
6.81	3.593	0.046

7.33	3.759	0.037
7.84	3.843	0.07
8.34	3.839	0.06
8.89	3.903	0.079
9.36	4.034	0.095
9.87	3.991	0.079
10.64	4.241	0.068
11.67	4.333	0.101

Figures	Table 2. and Fig. 6. The energy dependence of average number of prompt neutrons of ^{237}Np (n,f)
Location	

5. ***This paper includes input parameters for prompt-nubar calculations****

Title	Prompt-nubar Calculations for 53 Actinides
Author(s)	Reichard Q. Wright, Luiz Leal, R.M. Westfall
References Other Papers	6. V. M. Maslov et al., International Atomic Energy Agency (IAEA) reports INDC(BLR)-2–7, 9–11, 14, 15, and 21 (1995−2010), (IAEA, Vienna, Austria).
Value	Table 3. Prompt-nubar values (0.0253 eV)

Nuclide	MADNIX	ENDF/B-VII.1	% Diff
^{234}Np	2.6363	2.6323	0.15
^{235}Np	2.6536	2.6323	0.81
^{236}Np	2.7149	2.4000	13.1
^{237}Np	2.6370	2.6250	0.46
^{238}Np	2.7205	2.4700	10.1
^{239}Np	2.7005	2.6991	0.05

Table 4. Prompt-nubar comparison

Nuclide	MADNIX	Maslov	% Diff
^{236}Np	2.7149	2.7160	-0.04
^{237}Np	2.6370	2.6343	0.10
^{238}Np	2.7205	2.7350	-0.53

Figures	Table 3. Prompt-nubar values (0.0253 eV) Table 4. Prompt-nubar comparison Fig. 17. Prompt-nubar for ^{249}Cf, ^{242}Cm, and ^{237}Np
Location	Reactor and Nuclear Systems Division: ORNL/TM-2015/30

6.

Title	Review and Assessment of Neutron Cross Section and Nubar Covariances for Advanced Reactor Systems
Author(s)	VM Maslov, P Obložinský, and M Herman

References Other Papers	304. Khokhlov Yu. A., Ivanin I.A., In'kov V.I., et al. "Measurements results of average neutron multiplicity from neutron induced fission of actinides in 0.5-10 MeV energy range". Proc. Int. Conf. Nuclear Data for Science and Technology, Gatlinburg, USA, May 9-13, 1994, p. 272, J.K. Dickens (Ed.),ANS, 1994. 306. J.Frehaut, R. Bois, A. Bertin, Proc. Int. Conf. Nuclear Data for Science and Technology, Antwerpen, Belgium, September 6-10, 1982, p. 78, Reidel Publ. Co., Holland, 1983. 289. Malinovskyj V.V., Vorobjova V.G., Kuzminov B.D., Piksajkin V.M., Semjonova N.N., Valjavkin V.S., Solovjov S.M. Atomnaja Energija, 54, 209 (1983). 325. Veeser W., Phys. Rev. C 17, 385 (1978).
Value	Graph shown in Fig. 7.16
Figures	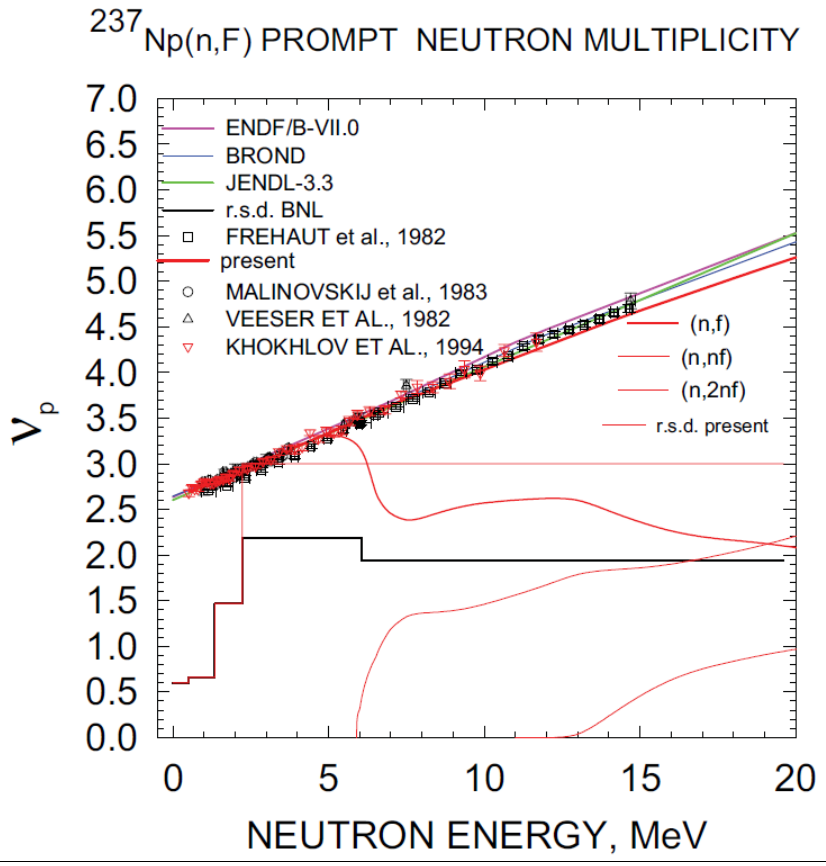
Location	Brookhaven National Laboratory – BNL-81884-2008-IR

7.

Title	Analysis of Np-237 ENDF for the Theoretical Interpretation of Critical Assembly Experiments
Author(s)	Bogdan Mihaila, Mark Chadwick, Robert MacFarlane, Toshihiko Kawano

<table>
<tr><td>References Other Papers</td><td>2. Veeser W., Phys. Rev. C 17, 385 (1978).
3. Frehaut J. et al., 1982 Antwerp, 78 (1982)
4. Malinovskii V.V. et al., Sov. At. Energy 54, 226 (1983)
5. Boikov G.S. et al., Phys. At Energy 57, 2047 (1994)
6. Mughabghab S.F. et al., Neutron Cross Sections, Vol. 1, Part B., Academic Press, INC. (1984).</td></tr>
<tr><td>Value</td><td>
<table>
<tr><td></td><td colspan="2">$\bar{\nu}_{total}$</td><td colspan="2">$\bar{\nu}_{delayed}$</td><td colspan="2">$\bar{\nu}_{prompt}$</td></tr>
<tr><td>Energy:</td><td>10^{-5} eV</td><td>1 MeV</td><td>10^{-5} eV</td><td>1 MeV</td><td>10^{-5} eV</td><td>1 MeV</td></tr>
<tr><td>Arthur et all</td><td>2.67120E+00</td><td>2.81900</td><td></td><td></td><td>2.65820E+00</td><td>2.8062</td></tr>
<tr><td>ENDF/B-VI</td><td>2.63581E+00</td><td>2.78562</td><td>1.08100E-02</td><td></td><td>2.62500E+00</td><td>2.7748</td></tr>
<tr><td>JENDL-3.2</td><td>2.54060E+00</td><td>2.68189</td><td>1.22000E-02</td><td></td><td>2.52840E+00</td><td>2.6697</td></tr>
<tr><td>JENDL-3.3</td><td>2.60140E+00</td><td>2.74780</td><td>1.20000E-02</td><td></td><td>2.58940E+00</td><td>2.7358</td></tr>
<tr><td>CENDL-2</td><td>2.52840E+00</td><td>2.70603</td><td>1.22000E-02</td><td></td><td>2.51620E+00</td><td>2.69389</td></tr>
</table>
</td></tr>
<tr><td>Figures</td><td>Fig. 4, Fig. 5, and Fig. 6 and Table II</td></tr>
<tr><td>Location</td><td>https://permalink.lanl.gov/object/tr?what=info:lanl-repo/lareport/LA-UR-04-7959

Theoretical Division, Los Alamos National Laboratory</td></tr>
</table>

8.

Title	Section 12.0 Useful Tables – Nuclear Weapons Frequently Asked Questions
Author(s)	
References Other Papers	
Value	Average neutron induced Nu_p (prompt neutrons/fission) • Incident neutron 1E-05 eV Nu_p = 2.625 • Incident neutron 1E+05 eV Nu_p = 2.640 • Incident neutron 1E+06 eV Nu_p = 2.775 • Incident neutron 4E+06 eV Nu_p = 3.224 • Incident neutron 2E+07 eV Nu_p = 5.521 • Incident neutron fission spectrum average Nu_p = 2.889
Figures	
Location	https://nuclearweaponarchive.org/Nwfaq/Nfaq12.html

9.

Title	Mesure de ν_p et E_γ, pour la fission de ^{232}Th, ^{235}U, et ^{237}Np induite par des neutrons d'energie comprise entre 1 et 15 MeV
Author(s)	J. Frehaut, A. Bertin, R. Bois
References Other Papers	10. Veeser W., Phys. Rev. C **17**, 385 (1978). 11. V.G. Vorobeva, B.D. Kuzminov, V.V. Malinovsky, N.M. Semenova, INDC (CCP) 177/L (1982) 39 et INDC (CCP) 156/G (1980).
Value	
Figures	
Location	https://link.springer.com/content/pdf/10.1007%2F978-94-009-7099-1_17.pdf

^{232}Th			^{235}U			^{237}Np		
$E_n \pm \Delta E_n$ (MeV)	$\bar{\nu}_p \pm \Delta\bar{\nu}_p$	$R \pm \Delta R$	$E_n \pm \Delta E_n$ (MeV)	$\bar{\nu}_p \pm \Delta\bar{\nu}_p$	$R \pm \Delta R$	$\bar{\nu}_p \pm \Delta\bar{\nu}_p$	$R \pm \Delta R$
2,37 ± 0,02	2,146 ± 0,012	0,834 ± 0,004	1,14 ± 0,24	2,475 ± 0,018	0,960 ± 0,005	2,706 ± 0,021	0,972 ± 0,006
2,59 ± 0,08	2,184 ± 0,021	0,831 ± 0,009	1,73 ± 0,19	2,557 ± 0,017	0,971 ± 0,004	2,759 ± 0,020	0,975 ± 0,005
2,93 ± 0,02	2,215 ± 0,015	0,830 ± 0,004	2,30 ± 0,16	2,610 ± 0,019	0,982 ± 0,005	2,842 ± 0,022	0,985 ± 0,006
3,39 ± 0,06	2,236 ± 0,014	0,827 ± 0,006	2,85 ± 0,14	2,685 ± 0,019	0,988 ± 0,005	2,932 ± 0,022	0,981 ± 0,006
3,91 ± 0,06	2,289 ± 0,015	0,843 ± 0,007	3,38 ± 0,13	2,751 ± 0,021	0,991 ± 0,005	3,015 ± 0,025	1,007 ± 0,006
4,43 ± 0,05	2,369 ± 0,015	0,859 ± 0,007	3,91 ± 0,12	2,816 ± 0,022	1,023 ± 0,006	3,084 ± 0,024	1,027 ± 0,006
4,49 ± 0,12	2,338 ± 0,020	0,851 ± 0,006	4,43 ± 0,11	2,919 ± 0,022	1,026 ± 0,006	3,193 ± 0,025	1,031 ± 0,007
4,95 ± 0,05	2,440 ± 0,015	0,852 ± 0,007	4,95 ± 0,10	2,981 ± 0,023	1,038 ± 0,006	3,272 ± 0,025	1,041 ± 0,007
5,13 ± 0,09	2,490 ± 0,017	0,857 ± 0,005	5,47 ± 0,09	3,084 ± 0,022	1,036 ± 0,006	3,368 ± 0,025	1,049 ± 0,007
5,47 ± 0,05	2,519 ± 0,018	0,851 ± 0,008	5,99 ± 0,09	3,170 ± 0,023	1,042 ± 0,006	3,437 ± 0,025	1,048 ± 0,007
5,72 ± 0,07	2,547 ± 0,023	0,865 ± 0,004	6,50 ± 0,08	3,278 ± 0,025	1,028 ± 0,007	3,536 ± 0,028	1,056 ± 0,008
5,98 ± 0,04	2,623 ± 0,020	0,866 ± 0,009	6,03 ± 0,34	3,173 ± 0,021	1,040 ± 0,006	3,451 ± 0,023	1,040 ± 0,007
6,27 ± 0,06	2,776 ± 0,014	0,844 ± 0,004	6,61 ± 0,29	3,311 ± 0,021	1,034 ± 0,006	3,560 ± 0,022	1,044 ± 0,006
6,49 ± 0,04	2,849 ± 0,018	0,864 ± 0,008	7,17 ± 0,25	3,387 ± 0,019	1,040 ± 0,005	3,621 ± 0,021	1,047 ± 0,006
6,82 ± 0,05	2,776 ± 0,024	0,864 ± 0,004	7,71 ± 0,23	3,460 ± 0,020	1,039 ± 0,005	3,708 ± 0,022	1,052 ± 0,005
7,00 ± 0,04	2,984 ± 0,021	0,852 ± 0,009	8,23 ± 0,21	3,537 ± 0,021	1,038 ± 0,005	3,785 ± 0,023	1,058 ± 0,006
7,51 ± 0,04	3,035 ± 0,023	0,852 ± 0,009	8,75 ± 0,19	3,609 ± 0,023	1,049 ± 0,005	3,882 ± 0,025	1,064 ± 0,005
6,90 ± 0,20	3,015 ± 0,011	0,841 ± 0,006	9,26 ± 0,17	3,681 ± 0,022	1,055 ± 0,005	3,988 ± 0,025	1,084 ± 0,005
7,35 ± 0,25	3,066 ± 0,014	0,853 ± 0,007	9,77 ± 0,16	3,768 ± 0,025	1,061 ± 0,005	4,029 ± 0,032	1,098 ± 0,007
7,88 ± 0,22	3,055 ± 0,013	0,860 ± 0,007	10,27 ± 0,15	3,843 ± 0,026	1,069 ± 0,005	4,121 ± 0,029	1,078 ± 0,006
8,39 ± 0,20	3,115 ± 0,012	0,867 ± 0,006	10,76 ± 0,14	3,903 ± 0,029	1,083 ± 0,006	4,179 ± 0,028	1,107 ± 0,005
8,90 ± 0,18	3,150 ± 0,014	0,882 ± 0,006	11,26 ± 0,14	3,993 ± 0,029	1,087 ± 0,005	4,287 ± 0,032	1,111 ± 0,006
9,40 ± 0,17	3,211 ± 0,016	0,889 ± 0,007	11,75 ± 0,13	4,068 ± 0,035	1,103 ± 0,006	4,364 ± 0,039	1,125 ± 0,006
9,90 ± 0,16	3,278 ± 0,015	0,887 ± 0,008	12,24 ± 0,12	4,118 ± 0,030	1,104 ± 0,005	4,418 ± 0,032	1,142 ± 0,006
10,39 ± 0,15	3,329 ± 0,017	0,900 ± 0,007	12,72 ± 0,12	4,215 ± 0,031	1,108 ± 0,006	4,469 ± 0,034	1,146 ± 0,006
10,88 ± 0,14	3,441 ± 0,020	0,896 ± 0,011	13,21 ± 0,11	4,279 ± 0,027	1,111 ± 0,005	4,524 ± 0,031	1,179 ± 0,005
11,37 ± 0,13	3,487 ± 0,016	0,923 ± 0,007	13,69 ± 0,11	4,365 ± 0,036	1,110 ± 0,005	4,586 ± 0,033	1,179 ± 0,006
11,86 ± 0,13	3,586 ± 0,021	0,932 ± 0,012	14,18 ± 0,10	4,408 ± 0,032	1,121 ± 0,006	4,655 ± 0,037	1,180 ± 0,007
12,34 ± 0,12	3,623 ± 0,019	0,935 ± 0,007	14,66 ± 0,10	4,459 ± 0,040	1,132 ± 0,007	4,702 ± 0,047	1,210 ± 0,009
12,85 ± 0,11	3,692 ± 0,018	0,944 ± 0,006					

10.

Title	Neutron Data Evaluation of ^{237}Np (2010)
Author(s)	V.M. Maslov, V.G. Pronyaev, N.A. Tetereva, A.M. Kolesov, K.I. Zolotarev, T. Granier, F.-J. Hambsch
References Other Papers	19. Poenitz, W.P., Aumeier, S.E., The simultaneous evaluation of the standards and other cross sections of importance for technology, Rep. ANL/NDM-139, Argonne Natl Lab., (1997). 127. Khokhlov,Yu. A., Ivanin, I.A., In'kov, V.I., et al., Measurements results of average neutron multiplicity from neutron induced fission of actinides in 0.5-10 MeV energy range, in Proc. 102 Int. Conf. Nuclear Data for Science and Technology, Gatlinburg, USA, 1994, J.K. Dickens (Ed.), ANS (1994) 272. 128.Veeser, W., Prompt neutrons from neutron-induced fission of 237Np. Phys. Rev. C17 (1978) 385. 129. Frehaut, J., Bois, R., Bertin, A., in Proc. Int. Conf. Nuclear Data for Science and Technology, Antwerpen, Belgium, 1982, Reidel Publ. Co., Holland (1983) 78.

	130. Mueler, R., Naqvi, A.A., Kaeppeler, F., Bao, Z.Y., Numerical results of a (2E,2V) measurements for fast neutron induced fission of 235U and 237Np, Rep. KFK-3068 (1980) 1. 131. Malinovskyj, V.V., Vorobjova, V.G., Kuzminov, B.D., Piksajkin, V.M., Semjonova, N.N., Valjavkin, V.S., Solovjov, S.M., On the divergence of the results of νp measurements for neutron-induced fission of 237Np, At. Energiya 54 (1983) 209. ****believed to be the same as Discrepancy of the Results of prompt-nubar measurements in the fission of 237Np nuclei by neutrons**** 132. Thierrens, H., Jacobs, E., D'Hondt, P., et al., The thermal neutron sub-barrier fission of 237Np, Nucl. Phys. A342 (1980) 229. 133. Boykov, G.S., Dmitriev, V.D., Svirin, M.I., Smirenkin, G.N., Neutron spectra in fission of 237Np by the neutrons with energies 2.9 and 14.7 MeV, Phys. At. Nucl. 57 (1994) 2047.
Value	TABLE 10.2. EVALUATED VALUES OF ν_p WITH LINEAR INTERPOLATION BETWEEN POINTS. UNCERTAINTIES ARE GIVEN FOR THE DIAGONAL OF COVARIANCE MATRIX. E_n eV | ν_p | Uncertainty % 1.0E-05 | 2.6343 | 5.9 0.0253 | 2.6343 | 5.9 5.0E+6 | 3.3470 | 1.0 8.0E+6 | 3.8610 | 1.5 1.5E+7 | 4.8094 | 1.3 2.0E+7 | 5.4880 | 12.1 TABLE 10.3. EVALUATED FIRST CHANCE ν_p –VALUES FOR ^{237,236,235}Np TARGET NUCLIDES. Target | ν_p^{th} | ν_p(E_n MeV) | ν_p(6 MeV) ^{237}Np | 2.619 | 2.950 (2.37) | 3.484 ^{236}Np | 2.922 | 2.869 (1.06) | 3.987 ^{235}Np | 2.818 | 2.908 (2.13) | 3.861
Figures	Fig. 10.1, Fig. 10.2,
Location	https://inis.iaea.org/collection/NCLCollectionStore/_Public/43/032/43032641.pdf?r=1&r=1

11.

Title	An Integrated System for Production of Neutronics and Photonics Calculational Constants Volume 15, Part B. THE LLL EVALUATED-NUCLEAR-BATA LIBRARY (ENDL): GRAPHS OFCROSS SECTIONS FROM THE LIBRARY
Author(s)	R.J. Howerton, D.E. Cullen, M.H. MacGregor, S.T. Perkins, and E.F. Plechaty,
References Other Papers	

Value	Not Listed in a Table, provided in a figure.
Figures	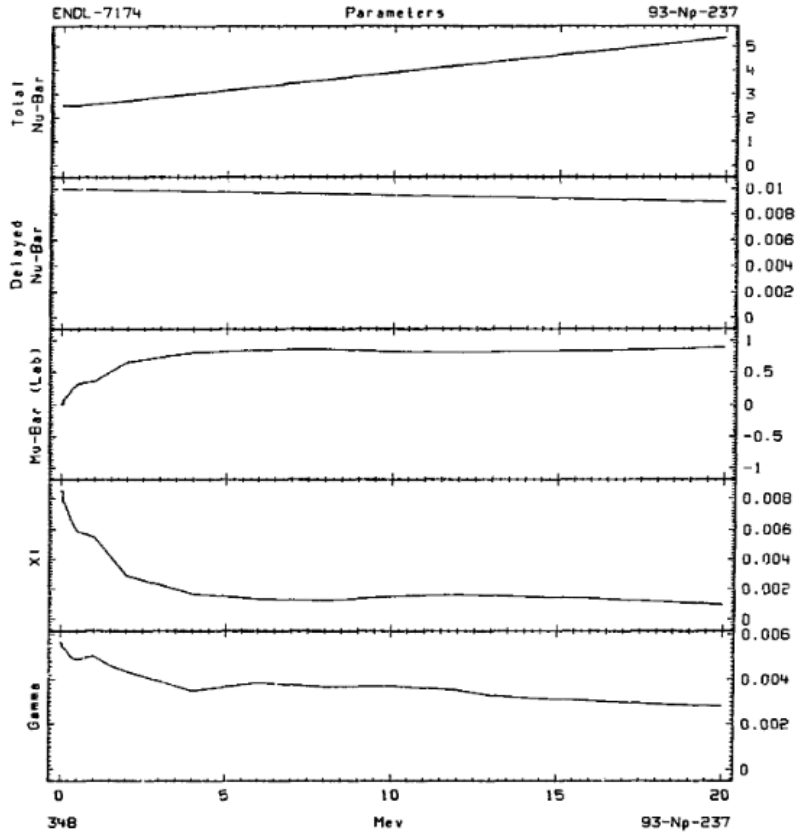
Location	Lawrence Livermore Laboratory Report No. UCRL-50400, 1976 (unpublished), Vol. 15, Part B. https://www.osti.gov/servlets/purl/6194637

12.

Title	Neutron Cross Sections, Vol. 1, Part B., Academic Press, INC. (1984).
Author(s)	Mughabghab S.F. et al.,
References Other Papers	
Value	Thermal Cross Sections: $\bar{\nu} = 2.525 \pm 0.016$
Figures	
Location	Page. 506 of Recommended-Thermal-Cross-Sections, RESONANCE PROPERTIES, and resonance parameters for Z=61-100

13.

Title	Measurements of Delayed-Neutron Yields from Thermal-Neutron-Induced Fission of 235U, 233U, 239Pu, and 237Np*
Author(s)	S. B. Borzakov, A. N. Andreev, E. Dermendjiev, A. Filip, W. I. Furman, Ts. Panteleev, I. Ruskov, Yu. S. Zamyatnin, and Sh. Zeinalov

References Other Papers	6. M. C. Brady and T. R. England, Nucl. Sci. Eng. **103**, 129 (1989). 14. S. B. Borzakov et al., in *Nuclear Data for Science and Technology, Trieste, 1997* (Bologna, 1997), Vol. 1, p. 497. 19. Sh. S. Zeinalov et al., Prepring No. R3-98-17, JINR (Dubna, 1998). 22. H. H. Saleh, T. A. Parish, and N. Shinohara, Nucl. Sci. Eng. **125**, 51 (1997). 23. A. N. Gudkov et al., At. Energ. **66**, 100 (1989). 24. G. Benedetti et al., Nucl. Sci. Eng. **80**, 379 (1982). 25. A. A. Malinkin et al., *Probl. At. Sci. and Tech. Phys. Nucl. Reactors* (1992), Part 3, p. 37. 26. V. M. Piksaikin et al., *XIV Workshop on Nuclear Fission, Obninsk,* 1998. 27. R. W. Waldo et al., Phys. Rev. C **23**, 1113 (1981).
Value	**Table 4.** The values of ν_d for ^{237}Np

$\nu_d \times 10^2$	Reference	Comment	$\nu_d \times 10^2$	Reference	Comment
1.25 ± 0.11	This work	Thermal neutrons	1.26 ± 0.07	[25]	Fast neutrons (1.3 MeV)
1.14 ± 0.11	[19]	Thermal neutrons	1.14 ± 0.12	[6]	Calculation
1.29 ± 0.04	[22]	Fast neutrons (144 keV)	1.07 ± 0.10	[27]	Fast neutrons
1.18 ± 0.13	[23]	Fast neutrons	1.00–1.14	[26]	0.4–1.2 MeV
1.22 ± 0.03	[24]	Fast neutrons			

Figures	Table 4. & Fig. 6.
Location	https://link.springer.com/content/pdf/10.1134%2F1.855663.pdf

14.

Title	Delayed Neutron Measurements from Neutron Induced Fission of ^{235}U, ^{233}U, ^{239}Pu, and ^{237}Np
Author(s)	S. B. Borzakov et al.
References Other Papers	9. R. J. Tuttle, Nucl. Sci. and Eng., 56, p. 37, 1975.
Value	$\nu_d = 1.01 \pm 0.15$
Figures	
Location	TA03-207 – Library: QC770.N473 (1997)

15.

Title	Mean Number of Neutrons From Fast Fission of 237Np
Author(s)	V. I. Lebedev and V. I. Kalashnikova
References Other Papers	[6.] Leachman, First International conference on the peaceful uses of atomic energy (Geneva, 1955). Selected reports of foreign scientists, Vol. 2 [in Russian] Moscow, Atomizdat, 1959, p. 282.
Value	ν (Np^{237}) = 2.96 ± 0.05 Fast Neutron Reactor: ν (Np^{237}) = 2.72 ± 0.15 Reference [6] – "Topsy" and "Jezebel" critical assemblies with mean neutron energy spectra of 1.40 and 1.67 MeV gave : ν (Np^{237} @ 1.40 MeV) = 2.81 ± 0.09 and : ν (Np^{237} @ 1.67 MeV) = 2.90 ± 0.04
Figures	
Location	https://link.springer.com/content/pdf/10.1007%2FBF01479937.pdf

16.

Title	Neutron spectra in fission of 237Np by the neutrons with energies 2.9 and 14.7 MeV
Author(s)	Boikov, G.S., Dmitriev, V.D., Svirin, M.I., Smirenkin, G.N.
References Other Papers	12. Malinovskii, V.V. Tarasko, M.Z., and Kuz'minov, B.D., *Vopr. At. Nauki Tekh., Ser.: Yad. Konstanty,* Moscow: TsNIIAtominform, 1985, no. 1, p. 24.
Value	

E_n, MeV	$\bar{\nu}_{exp}$	$\bar{\nu}$	$\bar{\nu}$ [12] **
2.9	2.98 ± 0.07	3.01 ± 0.07	3.03 ± 0.05
14.7	4.45 ± 0.08	4.52 ± 0.10	4.78 ± 0.10

Figures	
Location	TA03-207, Journal Stacks, Physics of Atomic Nuclei 57 (1994) p. 2047

17.

Title	The Number of Prompt Neutrons in the Fission of U-235, U-233, Th-233, and Np-237 by Fast Neutrons
Author(s)	B.D. Kuz'minov, L.S. Kutsaeva, and I.I. Bondarenko
References Other Papers	
Value	ν (E) = 2.72 ± 0.15
Figures	TABLE – Results of Measuring the Number of Prompt Neutrons
Location	https://link.springer.com/content/pdf/10.1007%2FBF02207351.pdf

18.

Title	Discrepancy of the Results of prompt-nubar measurements in the fission of 237Np nuclei by neutrons
Author(s)	V.V. Malinovsky, M.Z. Tarasko, B.D. Kuzminov
References Other Papers	1. Veeser W., Phys. Rev. C **17**, 385 (1978). 2. V.G. Vorobeva, B.D. Kuzminov, V.V. Malinovsky, N.M. Semenova, INDC (CCP) 177/L (1982) 39 et INDC (CCP) 156/G (1980). 3. Frehaut J. et al., 1982 Antwerp, 78 (1982)
Value	TABLE 1. Results of $\bar{\nu}_p$ Measurements in the Fission of ^{237}Np Nuclei by Neutrons

Neutron energy, MeV	Error in neutron energy (MeV)	$\bar{\nu}_p$	Statistical error
0,98	0,04	2,795	0,012
1,17	0,04	2,815	0,019
1,28	0,04	2,774	0,014
1,38	0,04	2,772	0,022
1,46	0,04	2,824	0,016
1,62	0,04	2,817	0,017
1,66	0,06	2,907 *	0,033
1,68	0,04	2,882	0,015
1,77	0,04	2,841	0,013
1,89	0,04	2,887	0,018
1,92	0,04	2,886	0,010
2,00	0,04	2,853	0,013
2,00	0,05	2,893 †	0,034
2,09	0,04	2,880	0,017
2,13	0,04	2,878	0,010
2,23	0,03	2,944	0,012
2,31	0,03	2,944	0,018
2,43	0,03	2,960	0,017
2,62	0,04	2,981	0,014
2,64	0,05	3,011 *	0,022
2,71	0,03	2,990	0,017
2,79	0,05	3,003 *	0,018
2,92	0,03	3,006	0,017
3,07	0,05	3,051 *	0,020
3,09	0,03	3,065	0,014
3,21	0,03	3,040	0,016
3,45	0,03	3,110	0,017
3,52	0,03	3,084	0,022
3,71	0,02	3,166	0,018
5,58	0,08	3,445	0,025
5,90	0,08	3,493	0,024

* Results of measurements obtained with a fission chamber containing a single neptunium layer.
† Measurements made with a spiral-shaped fission chamber.

Figures	
Location	https://link.springer.com/content/pdf/10.1007%2FBF01125717.pdf

19.

Title	Analysis of prompt fission neutron spectrum and multiplicity for ^{237}Np(n,f) in the frame of multi-modal Los Alamos model
Author(s)	Zheng Na, Ding Yi, Zhong Chun-Lai, Chen Jin-Xiang, and Fan Tie-Shuan
References Other Papers	[25] Malinovskyj V V, Vorobjova V G, Kuzminov B D, Piksajkin V M, Semjonova N N, Valjavkin V S and Solovjov S M 1983 At. Energ. 54 209 [26] Khokhlov Y A and Ivanin I A 1997 Proc. Int. Conf. on Nuclear Data for Science and Technology Trieste, Italy eds. Reffo G, Ventura A and Grandi C, Societa Italiana di Fisica, Bologna, Italy 1 667 [27] Frehaut J, Bertin A and Bois R 1983 Proc. Int. Conf. on Nuclear Data for Science and Technology Antwerp, Belgium (Dordrecht: Reidel) 17, p78
Value	"The total average prompt multiplicity calculated on the basis of the multi-modal multiplicities by using expressions (2) and (4) accords well with experimental data,[25-27] as can be seen in Fig. 8."
Figures	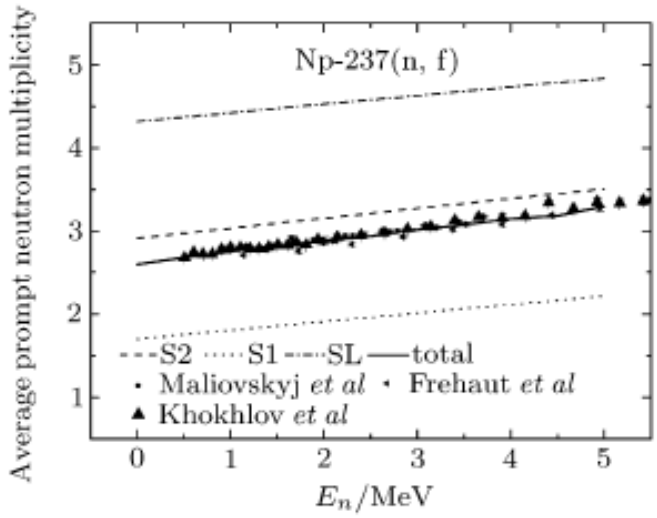 **Fig.8.** Average prompt fission neutron multiplicity (solid line) as a function of incident neutron energy, compared with the experiment data,[25−27] where contributions of three fission modes are also shown.
Location	2009 *Chinese Phys. B* **18** 1413

20.

Title	Improved Los Alamos model applied to the neutron induced fission of ^{235}U and ^{237}Np
Author(s)	G. Vladuca, Anabella Tudora
References Other Papers	Frehaut J, Bertin A and Bois R 1983 Proc. Int. Conf. on Nuclear Data for Science and Technology Antwerp, Belgium (Dordrecht: Reidel) 17, p78 Ohsawa, T., Hayashi, H., Ohtani, Y., 1997. In: Re€o, G., Ventura, A., Grandi C. (Eds.), Proc. Int. Conf. 434 G. Vladuca, A. Tudora / Annals of Nuclear

	Energy 28 (2001) 419±435 On Nuclear Data for Science and technology, ICTP Trieste, Italy (Italian Physical Society, Bologna) Part I, p.365. Ohsawa, T., Horiguchi, T., Hayashi, H., 1999. Nucl. Phys. A 653, 17±26.
Value	Table 3 Average prompt neutron multiplicity for the spontaneous fission of ^{236,235,234}U and ^{238,237,236,235}Np nuclei Nucleus U-236 U-235 U-234 Np-238 Np-237 Np-236 Np-235 $\bar{\nu}_p$ S.F. 1.7758 1.9068 1.9181 1.9308 2.1835 2.0520 2.0555
Figures	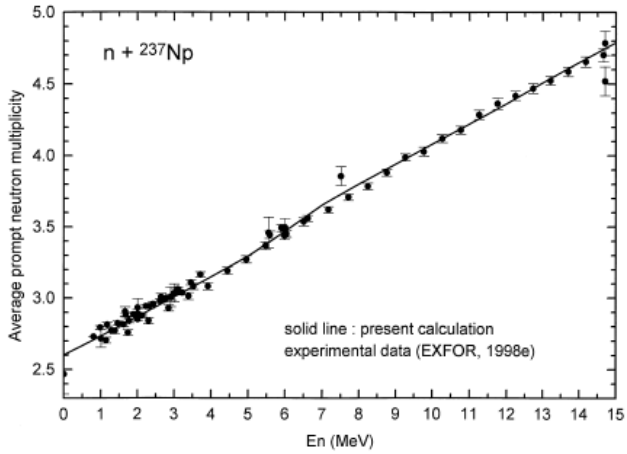 Fig. 5. Average prompt fission neutron multiplicity versus the incident neutron energy for the $n + ^{237}$Np reaction, present calculation and experimental data.
Location	Annals of Nuclear Energy 28 (2001) 419±435

21.

Title	Measurements of the Energy Dependence of the Mean Number of Prompt Neutrons in Neutron-Induced Fission of 237Np Nuclei
Author(s)	V.G. Vorobeva, B.D. Kuzminov, V.V. Malinovsky, N.M. Semenova
References Other Papers	[1] Neutron Standard Reference Data. Vienna, IAEA, 1974, p. 360. [2] Veeser L.R. – Phys. Rev., 1978, v.C17, p. 385.
Value	TABLE 2 Results of measuring the energy dependence of $\bar{\nu}_p$

E_n, MeV	$\pm \Delta E_n$, MeV	$\bar{\nu}_p$	$\pm \Delta \bar{\nu}_p$	E_n, MeV	$\pm \Delta E_n$, MeV	$\bar{\nu}_p$	$\pm \Delta \bar{\nu}_p$
0,98	0,04	2,8I6	0,034	2,23	0,03	2,966	0,034
I,I7	0,04	2,836	0,047	2,3I	0,03	2,966	0,038
I,28	0,04	2,795	0,035	2,43	0,03	2,983	0,036
I,38	0,04	2,793	0,039	2,62	0,04	3,004	0,037
I,46	0,04	2,846	0,036	2,7I	0,03	3,0I3	0,039
I,62	0,04	2,838	0,035	2,92	0,03	3,029	0,039
I,68	0,04	2,904	0,040	3,09	0,03	3,088	0,037
I,77	0,04	2,863	0,034	3,2I	0,03	3,063	0,039
I,89	0,04	2,909	0,037	3,45	0,03	3,I34	0,040
I,92	0,04	2,908	0,035	3,52	0,03	3,I08	0,042
2,00	0,04	2,875	0,034	3,7I	0,02	3,I90	0,042
2,09	0,04	2,902	0,036	5,58	0,08	3,47I	0,07I
2,I3	0,04	2,900	0,033	5,90	0,08	3,520	0,079

Figures	
Location	INDC (CCP) 177/L (1982) 39 et INDC (CCP) 156/G (1980)

22.

Title	Measurements of the average energy and multiplicity of prompt-fission neutrons from 238U(n,f) and 237Np(n,f) from 1 to 200 MeV
Author(s)	J. Taieb, T. Granier, T. Ethvignot, M. Devlin, R.C. Haight, R.O. Nelson, J.M. O'Donnell, and D. Rochman
References Other Papers	
Value	No Table of values, only Fig. 5. which compares the information to Frehaut
Figures	Fig. 5. Neutron multiplicity as a function of the kinetic energy of the neutron. Previously measured data are also shown.
Location	International Conference on Nuclear Data for Science and Technology 2007 DOI: 10.1051/ndata:07676

23.

Title	Multiplicities of Fission Neutrons*
Author(s)	B. C. Diven, H. C. Martin, R. F. Taschek, and J. Terrell
References Other Papers	
Value	Provides the methodology for how to calculate nubar
Figures	
Location	

24.

Title	ENDF/B-VIII.0
Author(s)	
References Other Papers	MT=456 Prompt Neutron Yields. Based on smooth curve through experimental data of Ma83,Ve78,Fr82, after renormalization for ENDF/B-VI standards. Results agree closely with values from Madland-Nix theory (Ma84). Fr82 J.Frehaut et al., Int.Conf.on Nucl.Data for Sci.& Tech., Antwerp, 6-10 Sept.1982, p.78. Ve78 L.Veeser et al., Phys.Rev.C17, 385 (1978). Ma83 V.V.Malinovsky et al., YK 1,50 (1983). Ma84 D.G.Madland, personal communication (1984).
Value	Incident Energy (eV) 1e-5 2.625 4e6 3.22425 7e6 3.677437 1.1e7 4.3248 1.2e7 4.4669 2e7 5.5207
Figures	
Location	JANIS - Incident neutron data / ENDF/B-VIII.0 / Np237 / MT=456 : nubar prompt / Neutron production

25.

Title	JEFF-3.3
Author(s)	P.Young,E.Arthur,F.Mann,T.Kawano
References Other Papers	
Value	Incident Energy (eV) 1e-5 2.625 4e6 3.22425 7e6 3.677437 1.1e7 4.3248 1.2e7 4.4669 2e7 5.5207
Figures	
Location	NNDC.bnl.gov

26.

Title	ENDF/B-VII.I
Author(s)	
References Other Papers	
Value	Incident Energy (eV) 1e-5 2.625 4e6 3.22425 7e6 3.677437 1.1e7 4.3248 1.2e7 4.4669 2e7 5.5207
Figures	
Location	

APPENDIX D

CONVERSION OF A *MCNP®6/6.2* OUTPUT TO A .GAM FILE

The *MCNP®6/6.2* radiation leakage information was obtained using a F1 tally for photons, where this tally measured the current across the surface. An energy bin distribution for the F1 tally is given by a file named 'MCNPbins.dat' which can be obtained in the GADRAS files. This file contained an energy bin structure that had a total of 1477 energy bins that needed to be converted from MeV to keV. GADRAS measures energy in units of MeV while *MCNP®6/6.2* measures energy in units of keV. The *MCNP®6/6.2* F1 tally table output provided the following information:

1. The first column shows the upper bound of the energy bin or the group in MeV.
2. The second column gives the corresponding leakage for the energy bin.
3. The third column is not needed for the gam file for GADRAS.

The first two columns of this table were needed to generate a .gam file. Pathway 1 for doing this consisted of copying this table into an Excel file and converting the first column back to keV, instead of MeV. Next, the energy bins from MCNP were manipulated to use the lower energy bound rather than the upper bound to reflect GADRAS preferences. This was done by shifting the leakage column up by one cell and typing 0 for the last empty bin in GADRAS.[40]

In order for the F1 tally table output to be readable by GADRAS, a gam file needed to be created. The process to generating a gam file using *MCNP®6/6.2* was as follows [40]:

1. Line 1 of the gam file has three entries;
    a. 1st entry: version number
    b. 2nd entry: model geometry (0=spherical, 1=cylindrical, 2=rectilinear)

c. 3rd entry: model extent

i. Spherical geometry: ignored (just enter 0)

ii. Cylindrical Geometry: cylinder length in cm

iii. Rectilinear geometry: slab surface area in cm^3

2. First line in GADRAS will always be " 0 0 0 " when importing a GAM file from a MCNP output.
3. Line 2 of the gam file has three entries;
   a. 1st entry: number of discrete gamma rays. The interface protocol between *MCNP®6* and GADRAS that is described in this document assumes that the radiation leakage is represented by leakage in a series of continuous energy groups and that no discrete gamma rays are represented, so the first number on the second line is ALWAYS 0.
   b. 2nd entry: number of energy groups for calculation. This is equal to the number of bins in the MCNPbins.dat file minus 1. So the value is 1476.
   c. 3rd entry: number of neutron energy groups. Since we are only interested in generating gamma spectra this number will ALWAYS be 0.
4. Line 2 is followed by 1477 lines in the gam file. These 1477 lines consist of two columns. The first column should be the lower energy boundaries of the energy bin in units of keV and the second column, shifted up by one, should give the total leakage within that energy group bin.

This process was streamlined using a Python script to perform the manipulations and write the .gam file for GADRAS. A simple geometry was tested with a 100 % ^{237}Np sample to confirm that the spectrum appeared as expected. Further work will need to be performed to verify if the

hot-spot simulations performed before are acceptable. This required obtaining photon data that varied with impurity, which due to timing could not be completed in the duration of the internship. However, the Python script and *MCNP®6/6.2* input structure were completed to make future efforts simpler. A basic input with a pure sphere was modeled, a hot spot geometry input was made, and a sphere with impurities distributed throughout.